PINSA, **67, A,** No. 1, January 2001, pp. 1-30

MECHANISM AND KINETICS OF ALLOYING AND NANOSTRUCTURE FORMATION BY MECHANICAL METHODS

S K PABI, J JOARDAR AND B S MURTY*

Department of Metallurgical and Materials Engineering, Indian Institute of Technology, Kharagpur-721 302 (India)

(Received 06 March 2000; Accepted 15 September 2000)

Nanocrystalline materials have become a subject of both scientific and industrial importance in the past one decade. The present paper reviews the work being carried out world over, on the synthesis of nanocrystalline metals, alloys, intermetallics and nanocomposites by mechanical means, in particular, by high energy ball milling process. Many high melting intermetallics, that are difficult to prepare by conventional processing techniques, could be easily synthesized in nanocrystalline state with homogeneous structure and composition by this route. The present understanding of the nature of these materials and the phase transitions induced during nanocrystallization are critically reviewed in the present paper.

Key Words: Nanocrystalline Materials; Nanocomposites; High Energy Ball Milling; Nanocrystalline Intermetallic Compounds; Mechanical Alloying; Mechanical Milling; Devitrification; Plastic Deformation

1 Introduction

Nanocrystalline materials (NCM) are solids composed of crystallites with characteristic size (at least on one dimension) of a few nanometers. The discovery of these materials by Gleiter[1] can be viewed as one of the most fascinating ones of the past decade. The importance of these materials can be easily gauged by the launch of the International Journals like Nanostructured Materials and Nanotechnology even when the field is in its infancy. A biannual International Conference Series on these materials has been launched in 1992 and the fifth one in the series is scheduled in 2000[2-6]. The importance of the field can be recognized by the large number of international conferences being held regularly on nanophase materials[7-17]. Various aspects of these materials have been reviewed by a number of investigators[1,18-25].

The NCMs can be zero (clusters), one (lamellar), two (filamentary) or three (equiaxed particles)-dimensional in nature (Fig. 1)[26,27] and can be obtained by a number of techniques as shown in Table I. These are the materials characterized by a large volume fraction of grain boundaries as shown schematically in Fig. 2. The fraction of atoms associated with the boundaries, C is given by $C=3t/d$, where t is the thickness of the boundary and d is the diameter of the nanocrystal. Thus, the volume fraction of atoms at the grain boundaries can be of the order of 50% for 5 nm grains and a mere 3% for 100nm grains (Fig. 3). A number of physical and mechanical properties of materials are significantly altered in the nanocrystalline state as shown in Table II[28]. Nanostructured materials can be synthesized starting from vapour (inert gas condensation, sputtering, plasma processing, vapour deposition), liquid (electrodeposition, rapid solidification) and solid state (high energy ball milling, sliding wear, spark erosion). Among the solid state techniques, high energy ball milling has become quite popular in recent years due to its simplicity, low capital cost, higher productivity and scalability (Table III). The synthesis of NCM by the mechanical routes (high energy ball milling, sliding wear, spark erosion, cold rolling as well as devitification of mechanically induced amorphous phases) will be reviewed in the present paper.

High energy ball milling technique has been developed in 1966 by Benjamin and his co-workers[29] at the INCO's Paul D Merica Research Laboratory as a part of the programme to produce oxide dispersion strengthened (ODS) Ni-base superalloys for gas turbine applications. NCMs can be synthesized either by high energy ball milling of elemental blends (known as mechanical alloying (MA)) or that of individual

* *Present Address:* National Research Institute for Metals, Tsukuba 305-0047, Japan.

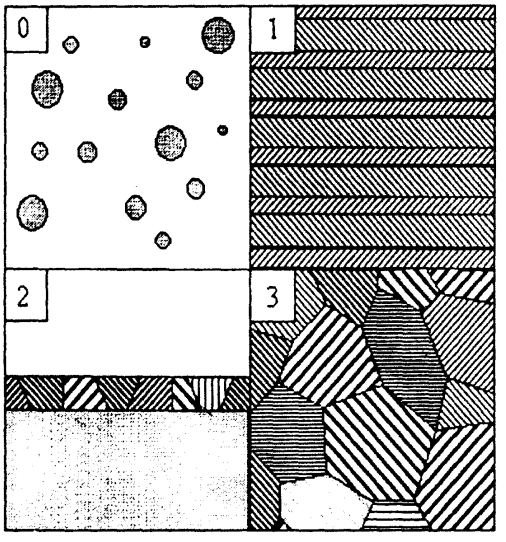

Fig. 1 Schematic of the four types of nanocrystalline materials[27]

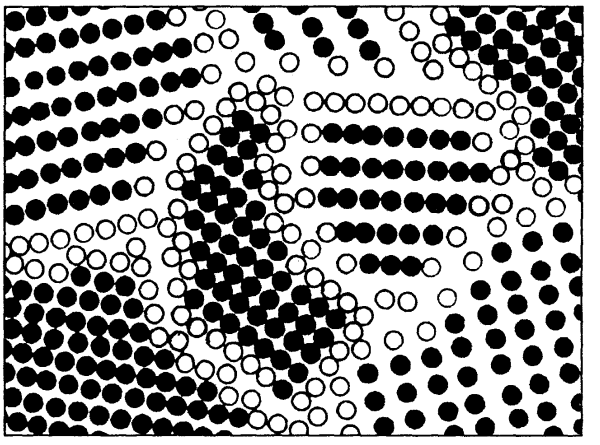

Fig. 2 Schematic representation of equiaxed nanocrystalline metal distinguishing between atoms associated with the individual grains (O) and those constituting grain boundary network (●)[1]

Table I

Classification of Nanocrystalline Materials

Dimensionality	Designation	Typical method(s) of synthesis
Three	Crystallites (equiaxed)	Gas condensation, mechanical alloying
Two	Filamentary	Chemical vapour deposition
One	Layered (lamellar)	Vapour deposition, electrode position
Zero	Clusters	Sol-gel method

Table II

Changes in the Properties in the Nanocrystalline State

Property	Change in the nanocrystalline state
Electrical	Higher conductivity in ceramics and magnetic nanocomposites
	Higher resistivity in metals
Magnetic	Increase in coercivity until a critical size
	Decrease in coercivity below a critical size leading to superparamagnetic behaviour
Mechanical	Increase in strength and hardness in metals and alloys
	Enhanced ductility, toughness and formability in ceramics and intermetallics
Optical	Blue shift of optical spectra in quantum-confined crystallites
	Increase in luminescent efficiency of semiconductors

Table III

Comparative Evaluation of MIGC, HEBM, Spray Conversion and Sol-Gel Methods (adopted and modified from[33])

Features	MIGC	HEBM	Spray conversion	Sol gel
Smallest grain size attainable	~2nm	~5nm	~10-20nm	~5nm
Contamination	<1%	High (unless milled with proper media under inert atmosphere)	High	High
Composition control	Sometimes difficult	Very good	Good	Difficult
Process control	Excellent	Good	Difficult	Difficult
Production rate (in laboratory unit)	Low	Good (~2kg/day)	Excellent	Good
Capital expenditure (in Indian Rupees)	>5 million	0.3-1 million	~4 million	~0.2 million
Production cost	High	Low	Low	Low
Possibility of scaling up	Difficult	Easy	Easy	Easy

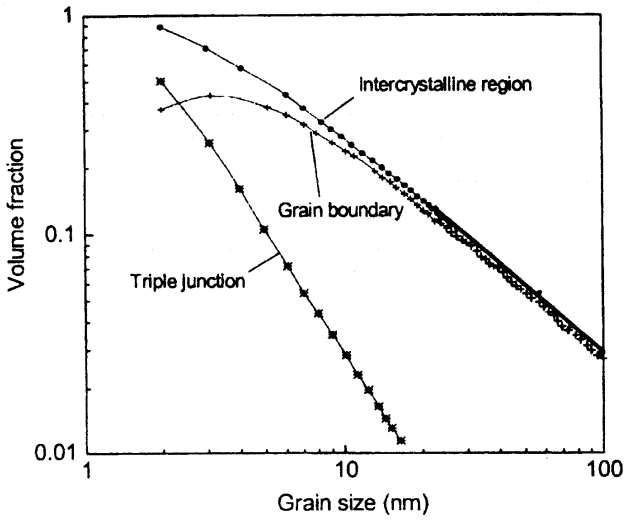

Fig. 3 Estimated volume fraction of grain boundaries, intercrystalline regions and triple junctions at various grain sizes, assuming grain boundary thickness of 1nm[22]

elements, alloys and intermetallics (known as mechanical milling (MM)). The formation NCMs during MA was first suggested by Koch *et al.*[30]. It was Fecht *et al.*[31], who have first synthesized elemental nanocrystals by high energy ball milling of their powders of a few micrometers in size. Over the past one decade, nanocrystalline metals, alloys, intermetallics, ceramics and nanocomposites have been synthesized in a number of systems by this technique[32-43]. Nanocrystals have also been synthesized through sliding wear[44], spark erosion[45] and severe plastic deformation[46], though these techniques have not become quite popular. Cold rolling has also been used to synthesize amorphous materials[47-50], that can be devitrified in a controlled fashion to yield nanocrystals.

2 High Energy Ball Milling

2.1 High Energy Ball Mills

MA/MM is usually carried out in high energy mills such as vibratory mills (Spex 8000 mixer/mill), planetary mills (Fritsch and Retsch mills) and attritor mills (Szegvari attritor). The energy transfer to the powder particles in these mills takes place by a shearing action or impact of the high velocity balls with the powder. An attritor was the first high energy ball mill used for MA by Benjamin[29]. The attritor, invented in 1922 by Szegvari for a quick dispersion of fine sulfur particles during the vulcanization of rubber, has a vertical cylindrical tank in which the powder and balls are charged. The movement of the balls and powder is achieved by the horizontally rotating impellers attached to a vertical shaft (Fig.4a)[32]. Set progressively at right angles to each other, the impellers energizes the grinding balls causing the size reduction of powder by impact. Due to the higher capacity of these attritor mills (Table IV), they are usually preferred in an industry rather than in research laboratories. The tumbler mills (Fig.4b)[32], which are traditionally used in mineral processing can also be used for MA, if their diameters are sufficiently large (of the order of meters) and if mills are operated close to the critical speed beyond which the balls stick to the inner walls of the mill. For large scale production, tumbler mills are more economical when compared to the attritor and other high energy ball mills[56]. Vibratory tube mills[57] are also used for pilot scale production in which a cylindrical container with the powder and ball charge is vibrated.

The laboratory mills, though have smaller capacities[58], offer a higher velocity for the balls[59-61]. Among the laboratory mills, Spex 8000 shaker mill and Fritsch Pulverisette have found wide use. In the Spex mill, most widely used in U.S.A., the vial containing the balls and powder is vibrated in three mutually perpendicular directions with amplitude of 50mm and a frequency of 20Hz. In the Fritsch planetary mill (P5 and P7), commonly used in the European countries, the disc and the vial mounted on the disc rotate in the opposite directions. This gives a centrifugal force to the balls (Fig.4c)[52]. In the basic models (P5 and P7) the speeds of the vial and disc can not be independently varied, however, this has been achieved in the modified versions (G5 and G7)[61-63]. It may be noted that even though the linear velocity of the balls in Fritsch mill is higher than that of Spex mill, the frequency of impacts is much more in the case of the Spex mill[59,60] which makes it a higher energy mill in comparison with the Fritsch mill. Due to the low energies of milling in the case of the attritor, it takes a longer period to achieve alloying when compared to the laboratory mills. It has been shown[64] that alloying in the case of Ti-Mg system takes place after 16h in the Spex mill, while the attritor took 100h to achieve the same result.

The Anutech uni-ball mill is the other high energy ball mill, which has found wide acceptance among the Australian investigators[51,65]. This mill consists

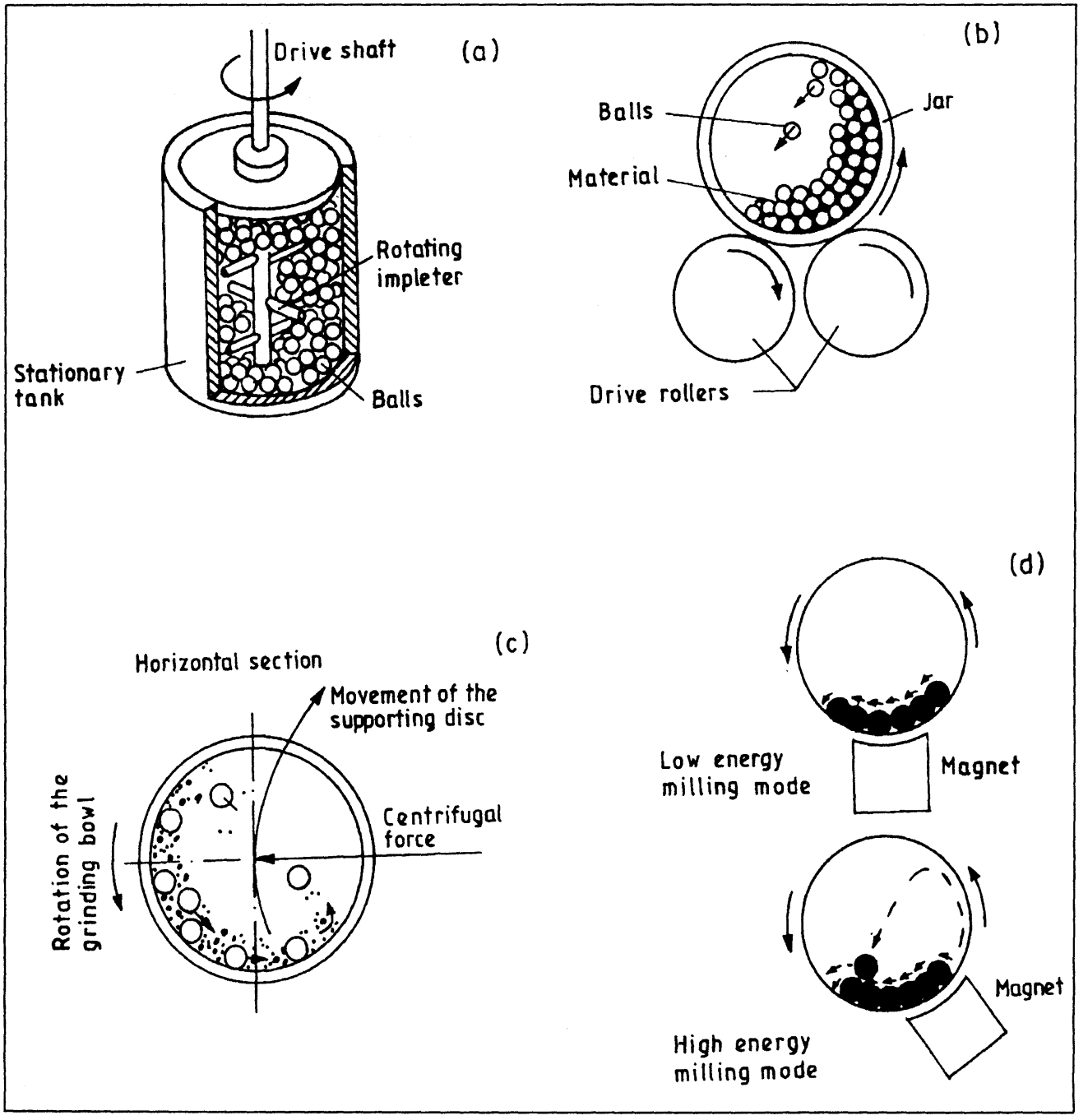

Fig. 4 Schematic of the milling processes in some of the ball mills (a) attritor, (b) tumbler mill, (c) Planetary ball mill (P-5) and (d) uni-ball mill

Table IV
Comparison of Various High Energy Ball Mills

Type of Mill	Capacity[52]	Ball velocity (m/s)	Reference
Mixer Mills	up to 2x20 g	<3.9	53
Planetary Mills	up to 4x250 g	<11.24	54,55
Attritor Mills	0 5-100 kg	<0.8	53
Uni Ball Mill	up to 4x2000 g	–	-

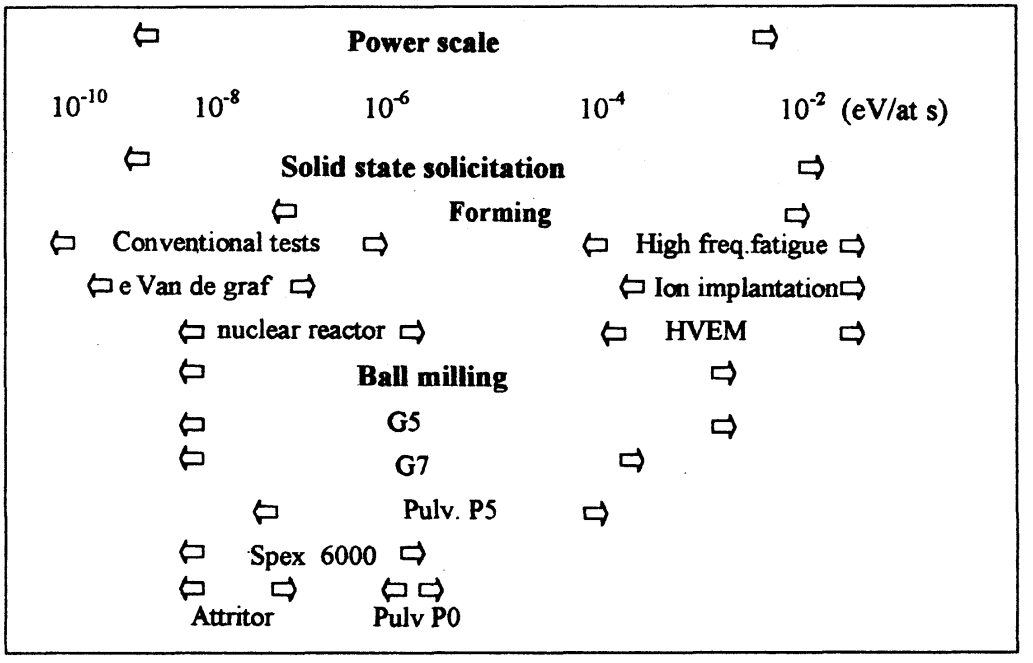

Fig. 5 Injected power levels in various mills[62, 71]

of a stainless steel horizontal cell with hardened steel balls. The movement of balls is confined to the vertical plane by the cell walls and is controlled by external magnetic field, whose intensity and direction can be adjusted. Depending on the position of the magnet, the mill can run in either high energy mode (impact prominent) or in low energy mode (shear prominent) (Fig. 4d)[51]. Another interesting feature of this mill is that the impact velocity and frequency can be independently controlled[51], which is not usually possible in the other mills unless some modifications are incorporated[57,63]. In addition to the above mills, several other mills such as Fritsch pulverisette P0 (single large ball in a vibrating frame mill)[66], rod mill[67], modified rod mill[68] and other specially designed mills[69,70] have been used for MA/MM. The capacities and linear velocities of the balls in various high energy ball mills are compared in Table IV. Fig. 5 compares the injected power levels in various mills[62,71].

2.2 Milling Parameters

Though the ultimate nanocrystalline grain sizes reported by high energy ball mills[72-74] and conventional low energy ball mills[75] are quite similar, the kinetics of nanocrystalline phase formation during MA/MM depend on the energy transferred to the powder ingredients from the balls during milling. The energy transfer is governed by various parameters *e.g.*, the type/design of the mill, milling speed, type, size and size distribution of the balls, ball to powder weight ratio (BPR), extent of filling of the vial, temperature of milling, grinding media and the milling atmosphere and finally the duration of milling. The kinetic energy of the balls will be higher with higher speeds of milling and with heavier balls (*e.g.* tungsten carbide (WC) better than steel). Joardar *et al.*,[76] have recently shown that nanocrystalline NiAl formation and its disordering tendency during MA are enhanced with increasing milling intensity. It has also been reported recently[77], that the reaction rate for the formation of nanocrystalline TiC during MA increases exponentially with the density of the balls. The size and size distribution and the number of the balls should be so chosen as to achieve optimum packing of the vial. Too dense packing of the balls decreases the mean free path of the ball, while loose packing minimizes the collision frequency. BPR of 5 to 10 is widely used and is found to be effective.

2.3 Contamination during Milling

Most of the MA work reported so far has been carried out using stainless steel (SS) or hardened chrome steel (CS) milling media (balls and container). These can introduce large amount of Fe contamination into the milled powder. It has been shown during the synthesis of NiAl from Ni and Al blend using SS milling media that the Fe contamination is to

the tune of about 18at.%[78]. However, with CS milling media (having better wear resistance than SS), the contamination level was ~5at.%[78]. The level of contamination not only depends on the milling media but also on other milling conditions such as the type of mill and milling speed etc. Contamination levels are expected to be more in high energy ball mills such as Spex mill. In order to minimize contamination, less energetic mills such as the vibratory mill may be used[32]. Contamination can be avoided by milling the powders with a milling media made up of the same material as that of the powders being milled[32]. However, the proposal is difficult to put into reality in many cases.

It has been shown recently[78-80] that Fe contamination from milling media can be a blessing in disguise. During the MA of elemental blend of Ni and Al, it was observed that completely disordered (long range order parameter, S=0) nanocrystalline NiAl forms when milled with SS media, while partially ordered (S=0.55) NiAl forms when milled in tungsten carbide[78]. Milling with CS media has resulted in NiAl having an intermediate value of S (0.48)[78]. Fig. 6[81] shows the X-ray diffraction (XRD) patterns of Ni and Al powder mixture of $Al_{75}Ni_{25}$ composition milled in Fritsch Pulverisette (P-5) at 300rpm for 30h using SS and WC milling media. The presence of (100) superlattice reflection of NiAl can be clearly seen (indicated by arrowhead in the figure) in the case of WC, while it is absent when milled in SS. In recent years, it has been argued that some ductility can be introduced into the otherwise brittle intermetallics by grain refinement[82] and/or by the introduction of disorder[83]. Fe is known to reduce the ordering energy of NiAl[83,84]. Thus, it is not surprising that Fe contamination during milling has resulted in the formation of disordered NiAl[78,81]. The above results suggest that Fe contamination from milling media may be helpful in improving the formability in some otherwise brittle aluminides.

Another example of the usefulness of Fe contamination was observed during MA of Cu-Ni elemental blends[79]. Complete alloying and the formation of solid solution was observed when an elemental blend of $Cu_{50}Ni_{50}$ was milled in Fritsch Pulverisette (P-5) at 300rpm for 20h in SS and CS milling media, while no alloying was observed when milled in WC under identical conditions (Fig. 7)[79]. Interestingly, in the case of CS and SS milling media, the Cu and Ni crystallites reached nanocrystalline state (<20nm) within 10h of milling, while in the case of WC media they remained coarse (>100nm) even after 20h of milling. This could be attributed to the change in the deformation characteristics of Cu and Ni due to Fe contamination during milling in SS and CS media. In fact Pabi *et al.*,[85] have recently shown that nanocrystallization is a prerequisite for alloying during high energy ball milling at least in slow diffusing systems such as Cu-Ni.

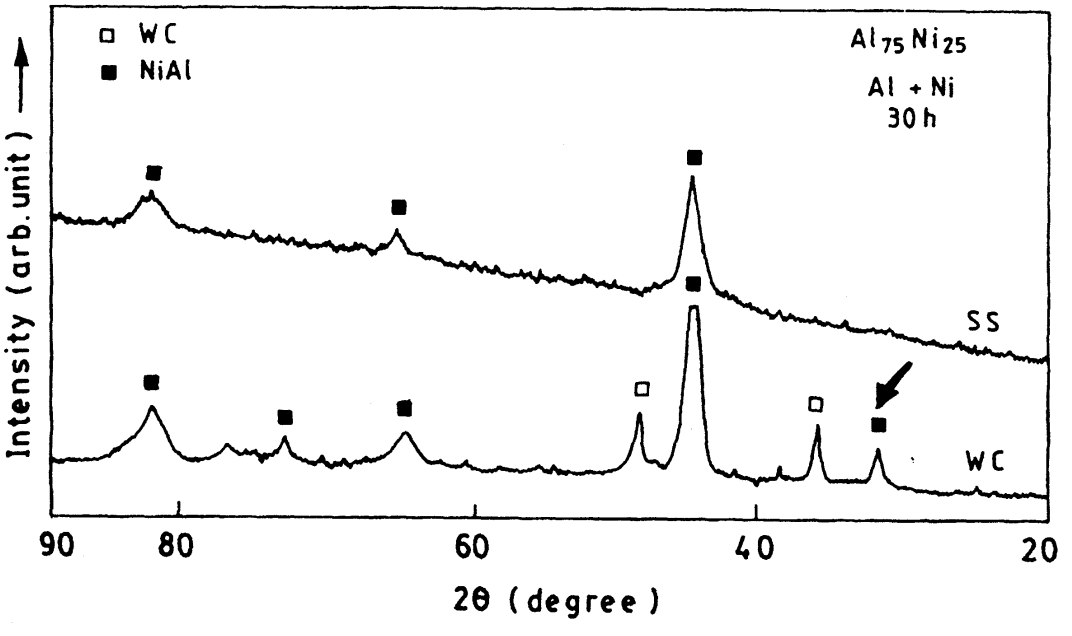

Fig. 6 Influence of WC and SS grinding media on the ordering characteristics of mechanically alloyed NiAl

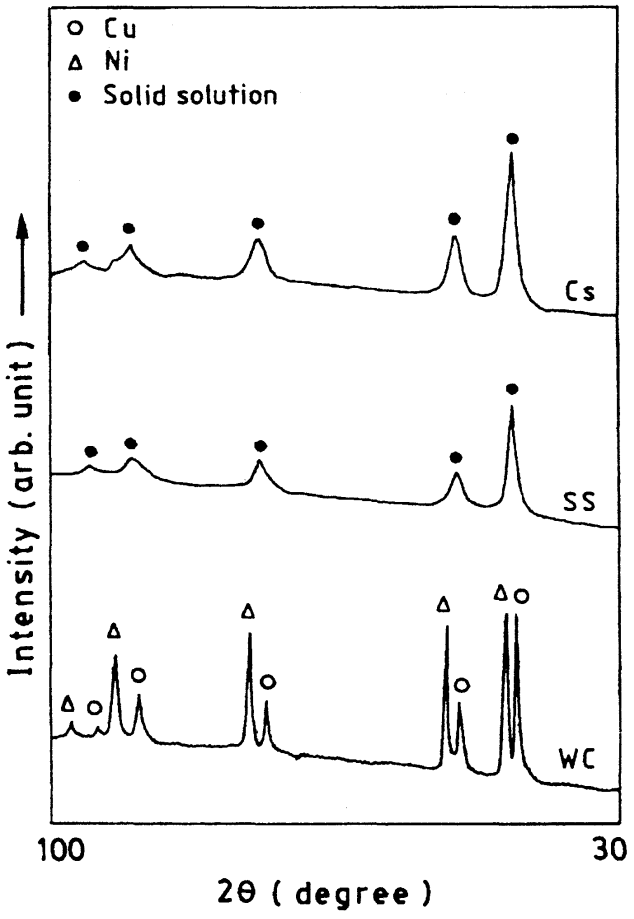

Fig. 7 Influence of grinding media on the alloying behaviour during MA of $Cu_{50}Ni_{50}$ elemental blend

2.4 Temperature of Milling

High energy ball milling is characterized by repeated cold welding and fragmentation of the powder ingredients. The extent of welding and fracturing is decided by the deformation behaviour of the powder and the temperature at the point of ball-powder-ball impact. Thus, the kinetics of nanocrystal formation during milling is expected to be a function of the milling temperature. Indeed the milling time at which a given nanocrystalline grain size was attained in TiNi intermetallic was found to be a function of milling temperature[86]. Shen and Koch[87] have observed smaller crystallite size for Cu and Ni when milled at 188K when compared to those milled at room temperature. The crystallite size of CoZr intermetallic was also smaller at low milling temperature[88]. Milling at subzero temperatures prevents excessive welding, while fracturing is favoured due to the change in the deformation characteristics of the powder[89] at low temperatures.

There have been a number of reports wherein the macroscopic temperature of the mill has been measured. Davis[90] and McDermott[91] have measured the maximum temperature of the Spex mill to be 323K (313K without balls) and concluded that most of the heat comes from motor and bearings. Kimura and Kimura[92] reported a maximum macroscopic temperature of 445K in the attritor. Borzov and Kaputkin[93] have measured a temperature in the range of 373-488K for attritor using SiC and diamond sensors. Substantial temperature rise (120K) is also reported by Kuhn *et al.*,[53] in vibratory mills. Thus the macroscopic temperature during mill appears to be low and sensitive to the mill design[94,95].

However, the microscopic temperature of the powder just after the impact can be quite high. In fact, Yermakov *et al.*,[96,97] have attributed amorphization during milling to the local melting and rapid solidification of the powders. As it is not practically feasible to measure the microscopic temperature rise at the point of ball-powder-ball impact during milling, investigators have taken recourse to two approaches for its estimation. One of the approaches being to ascertain it on the basis of appropriate models and the other being to infer from the structural/ microstructural changes during milling. However, there can be large temperature rise due to some exothermic reactions during milling. But this is not considered in these models.

Assuming that particles trapped between colliding balls (head-on collision assumed) deform by localized shear, Schwarz and Koch[55] estimated a microscopic temperature rise of about 40K for $Ni_{32}Ti_{68}$ and $Ni_{45}Nb_{55}$ powders in a Spex mill. Davis and Koch[98] calculated the ball velocities and used the expression and materials of Schwarz and Koch[55] to predict a raise in temperature ΔT of $\leq$112K. They[98] have also estimated the maximum ΔT to be about 350K. Maurice and Courtney[99] have also developed an expression for the adiabatic temperature rise during milling by modelling the deformation of powder as equivalent to microforging. However, they assumed ΔT to be low such that the material is in the cold working regime. Magini *et al.*,[100] have also calculated the adiabatic temperature in a planetary mill and reported the maximum temperature to be of the order of 400K after calculating the amount of powder trapped between the balls assuming a Hertzian collision. Bhattacharya and Arzt[101] calculated the contact

temperature of the powder compact surfaces, assuming Hertzian elastic collisions, which are higher (623K) than those calculated by others. However, they show a rapid decrease of the temperature to ambient temperature at the center of the compact. Davis and Koch[98] calculated the ΔT due to sliding friction to be very low ($\leq$10K). Miller *et al.*,[102] used microsecond time resolved radiometry to observe a temperature rise during impact on various materials. They observed ΔT of the order of about 400K.

In view of the difficulties in modelling of the temperature rise during milling, the microstructural changes occurring during ball milling provides a better alternative for realistic estimation. The observation of deformation bands and slip lines by optical microscopy[103] and the high dislocation densities and deformation bands seen in transmission electron microscopy[104] indicate that the microscopic temperatures are much below the recrystallization temperature. However, in some cases it is reported[92,105] that the temperature is above the crystallization temperature of the amorphous phase. Davis and Koch[97] studied the tempering of martensite in Fe-1.2%C steel during ball milling and concluded that the maximum microscopic temperature to be about 548K. Davis and Koch[98] have also milled Bi powder and concluded that the temperature of milling is below the melting point of Bi (544K). The milling temperature obtained by both calculations and experiments is compiled in Table V. The results suggest that there is only a moderate temperature rise at the point of ball-powder impact during milling, and the possibility of local melting can be ruled out.

Table V
Estimated Temperature Rise (ΔT) during Milling

Method of Estimation	ΔT (K)	Reference
Calculation	$\leq$ 10	98
	40	54
	130	99
	$\leq$ 350	98
	350	101
	400	100
Experimentation	50	90,91
	120	52
	100-215	93
	172	92
	< 271	98
	400	102

3 Nanocrystalline Phases by High Energy Ball Milling

3.1 Nanocrystalline Metals

Nanocrystalline structures were obtained by high energy ball milling of a number of elemental powders such as Cr, Nb, W, Hf, Zr and Co[106], Fe[107,108], Ni[109], Ag[110], Si[111,112] and graphite[113,114]. The crystallite sizes of the nanocrystals obtained by MA/MM are usually calculated from X-ray peak broadening after eliminating the strain and instrumental broadening constituents using standard methods[115,116]. TEM and HREM results have confirmed the nanocrystalline nature of these milled elements[72]. The initial results have shown an indication that the minimum crystallite size obtained by MM varies inversely with the melting point of the elements. It was argued[106] that in case of elements with low melting points, the tendency for cold welding dominates, resulting in larger crystallite sizes. Very recently, Koch[41] has compiled the minimum crystallite sizes reported so far for various elements by MM (Fig. 8). The figure clearly brings out the fact that for fcc elements having lower melting points (Al, Ag, Cu and Ni) the minimum crystallite size varies inversely with their melting point[74]. However, in case of bcc, hcp elements[72,73] and fcc elements with higher melting points (melting point of Pd)[74], the minimum crystallite size is virtually insensitive to their melting points. Thus, the understanding of the reasons for the minimum crystallite size is presently in a primitive stage. However, the fact that similar crystallite sizes were

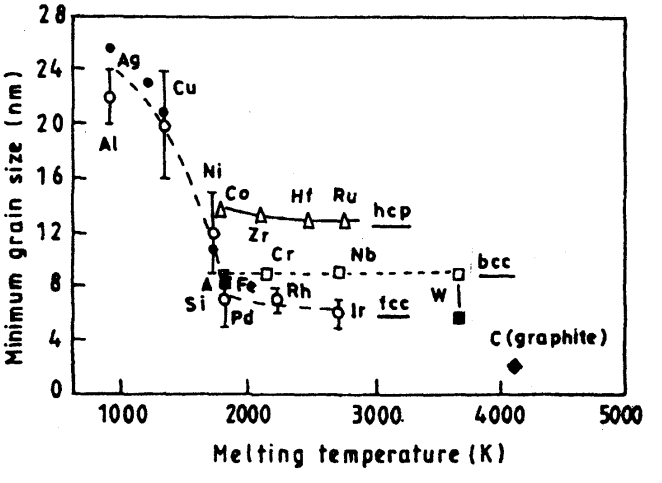

Fig. 8Effect of melting temperatures on the minimum crystallite sizes of various elements as attained by MM[41]

obtained both in conventional ball mills[75] as well as in the high energy ball mills suggests that it is the total strain, rather than the milling energy, that decides the minimum attainable grain size by MM.

The phenomenology of the development of nanocrystalline microstructure during high energy ball milling as summarized by Fecht[40] consists of three stages. In the first stage, deformation localization occurs in shear bands containing high dislocation density. In the second stage, dislocation annihilation/ recombination/rearrangement occurs to form cell/ subgrain structure in nanoscale and further milling extends this structure throughout the sample. In the third stage, the orientation of subgrains becomes random. It has been suggested that the ultimate grain size achievable is determined by the minimum grain size that can sustain dislocation pile-up within the grain and the rate of recovery during milling[74]. This means that the minimum crystallite size should be inversely proportional to the hardness[117]. A decreasing crystallite size with solute concentration has been observed in a number of alloy systems which exhibit solution hardening such as Cu(Fe)[118,119] Ti (Cu), Nb(Cu), Cu(Ni) and Cu(Co)[119]. The grain size of Ni(Co), where the hardness does not change significantly on alloying does not show any appreciable change during MA[87]. Similarly, an increase in grain size has also been observed in systems showing solid solution softening such as Ni(Cu), Fe(Cu) and Cr(Cu)[118].

3.2 Solid Solutions

3.2.1 Extension of Solid Solubility

Nanocrystalline solid solutions have been synthesized in a number of systems by MA of elemental powder mixtures such as Ti-Si[120], Ti-Ni, Ti-Cu[121], Ti-Mg[65] and Ti-Al[122,123]. Shen and Koch[119] have recently shown the formation of nanocrystalline solid solutions in Ti-Cu (0-8at.%Cu), Nb-Cu (0-20at.%Cu), Ni-Cu (0-50at.%Cu), Cr-Cu (0-20at.%Cu), Fe-Cu (0-15at.%Cu), Cu-Ni (0-50at.%Ni), Cu-Fe (0-50at.%Fe) and Cu-Co (0-50at.%Co) systems. They suggested that the solid solution hardening or softening is mainly governed by the hardening or softening of the grain boundaries. The extension of terminal solid solubility by MA has not been studied thoroughly so far, as the emphasis of most of the investigators was more either on the ODS alloys or on amorphization. The limited data available on the extension of terminal solid solubility achieved in different alloy systems by MA is shown in Table VI. The formation of solid solution in the entire composition range in the eutectic Ag-Cu system[125] has highlighted the potential of MA in achieving large extensions of terminal solid solubilities even in systems with positive enthalpies of mixing in the solid state. This is supported by the results of Suryanarayana and Froes[65], wherein a terminal solid solubility of 6at.% of Mg in Ti has been achieved by MA while these elements are immiscible in the solid state under equilibrium conditions. They have attributed this extension of solid solubility to the nanocrystalline structure formed during MA. The large volume fraction of grain boundaries present in the nanocrystalline state are expected to enhance the solid solubility in these materials. Murty *et al.*,[121] could show in Ti-Ni and Ti-Cu systems that the extension of solid solubility in these systems is limited by the onset of amorphization. In another report, Murty and Pabi[141] could correlate the limit of extension of solid solubility of NiAl during MA to its crystallite size. Thus, MA can be used very effectively to extend the solid solubility of one element in the other so as to obtain stronger alloys.

3.2.2 Alloying in Immiscible Systems

In the initial stages of development of MA, Benjamin[103] could demonstrate the formation of homogeneous mixtures of Fe-Cu and Cu-Pb by MA. Later, a significant solid solubility was reported in Fe-Cu system by MA[119,142-148]. Alloying has also been reported in Cu-W[149,150], Cu-V[151,152], Cu-Ta[153-155] and Cu-Co[156-158] systems by MA. Significantly, Huang *et al.*,[159] have reported continuous series of solid solutions in Cu-Co system. Alloying in liquid immiscible systems by MA is an interesting phenomenon and there have been efforts to understand the driving force for such a behaviour during high energy ball milling. Yavari *et al.*,[143,160] have attributed this to the capillarity effect in the nanocrystalline state. They argued that high energy ball milling results in the formation of small fragments with tip radii of the order of 1nm. The capillarity pressure at these tips forces the atoms on these fragments to dissolve. Gente *et al.*,[158] and Huang *et al.*,[159] have proposed that the formation of homogeneous solid solution is energetically more favoured when the crystallite size of the constituents is reduced below a critical size which is of the order of 1-2nm. Murty *et al.*,[79] Pabi *et al.*,[85] and Huang *et al.*,[161-163] have shown that

Table VI
Extension of Terminal Solid Solubility by MA

Solvent	Solute	Solid Solubility at room temperature (at %)		
		Equilibrium[124]	MA	Reference
Ag	Cu	0.3	100.0	125
	Ni	0.7	3.8	126
Al	Cr	0.0	5.0	127
	Fe	0.0	4.5	126
	Mg	2.1	23.0	126
	Mn	0.0	18.5	128
	Nb	0.0	25.30	126
	Ti	0.0	6.0	122
	Zr	0.0	9.1	126
Cd	Zn	0.0	50.0	129
Co	C	0.0	6.0	130
	Cr	0.0	40.0	131
	V	9.1	33.0	131
	Zr	0.0	5.0	131
Cr	Co	9.0	40.0	131
	Cu	0.0	20.0	119
Cu	Co	0.0	90.0	119,132
	Fe	0.0	50.0	119
	Hg	0.0	70.0	129
	Zn	30.0	50.0	80
Fe	Al	18.5	50.0	133
	Cu	0.0	15.0	119
	Mg	0.0	20.0	134
	Si	9.0	27.5	135,136
Mg	Ti	0.0	4.2	126
Mn	Co	4.0	50.0	131
Nb	Al	21.5	60.0	126
	Cu	0.0	20.0	119
	Ni	7.0	10.0	129
Ni	Ag	2.0	9.0	126
	Al	10.0	27.0	129
	C	0.0	12.0	130
	Nb	6.0	15.0	137
Ti	Al	36.0	55.0	138
	Cu	0.0	8.0	119
	Mg	2.9	60.0	65,139
V	Co	7.0	40.0	131
Zr	Al	0.5	15.0	140
	Co	0.0	4.0	131

nanocrystallization is a prerequisite for MA in immiscible or partially miscible systems.

3.3 Nanocrystalline Intermetallic Compounds

The intermetallics constitute some of the most technologically prospective engineering materials. This stems from their novel attributes such as excellent high temperature strength and thermal stability apart from the high corrosion/oxidation resistance and unique electrical and magnetic properties. However, the high melting temperatures and the poor formability of the intermetallics poses a major impediment to their conventional processing. Under this perspective, MA has been envisaged as an extremely promising solution. Over the past one decade, a considerable volume of work has been reported on the synthesis of a large number of intermetallic compounds through MA[42]. The possibility of producing these intermetallics in the nanocrystalline state by MA (Fig. 9a and b) has increased the popularity of this technique, as it can induce some formability in these otherwise brittle materials[164]. Fig. 10 shows that the increase in hardness is quite significant (by 4 to 5 orders) in case of metals on nanocrystallization[165], while in

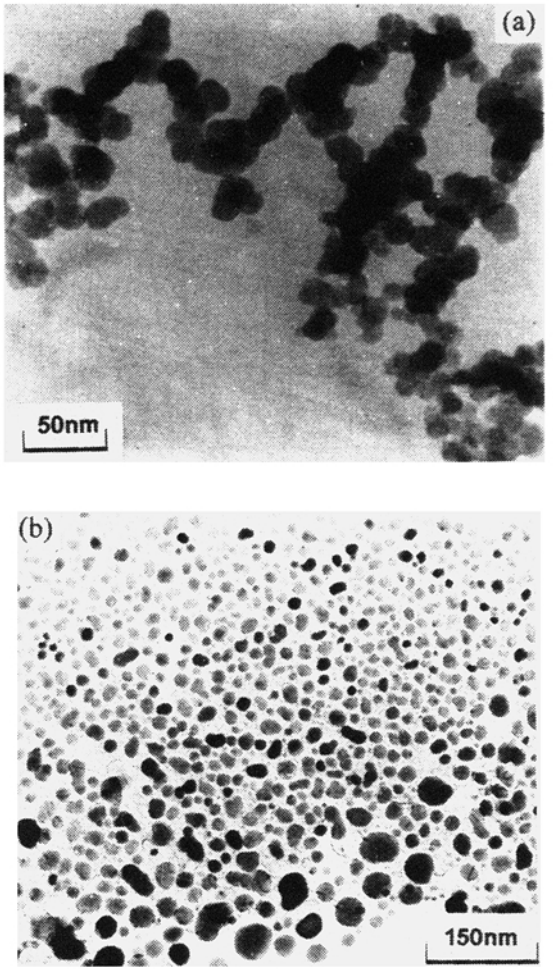

Fig. 9 TEM images of nanocrystalline (a) NiAl and (b) NiSi crystallites

case of intermetallics (Nb_3Sn) it is quite marginal (10-20%)[39]. Dymek *et al.*,[166] have demonstrated sufficient compressive ductility (>11.5%) in fine grained (<1μm) NiAl. Jain and Christman[167] have shown that nanocrystalline FeAl (Fe-28Al-2Cr crystallites of 80nm) is brittle in tension, but is superplastic in compression. The bulk of these efforts have been on the aluminides and to some extent on the silicides.

3.3.1 Aluminides

Overwhelming interest in the MA of nanocrystalline aluminides has been instigated by their possible applications in aerospace and automotive industries owing to their high specific strength and corrosion/ oxidation resistance at elevated temperatures. Among all aluminides, MA of Ni, Ti and Fe aluminides have so far received major attention.

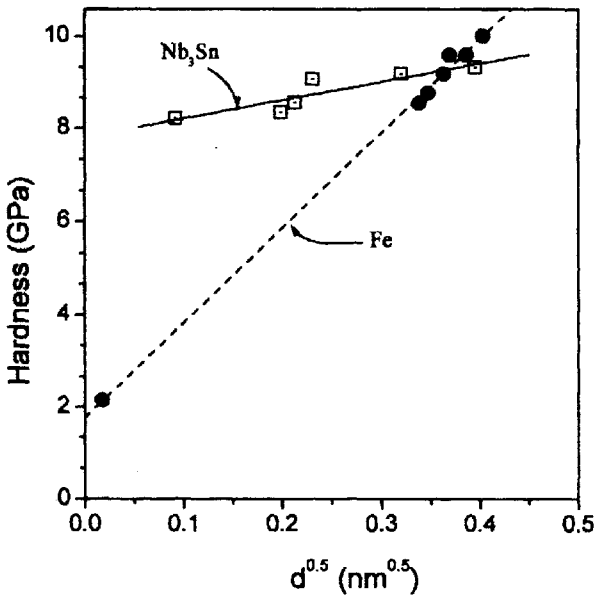

Fig. 10 Variation in hardness with $d^{-1/2}$ for Fe and Nb_3Sn, where d=average grain diameter[39,165]

Ni-Aluminides: The formation of nanocrystalline Ni-aluminides, such as $NiAl_3$, NiAl and Ni_3Al through MA has been established at various compositions in the binary Ni_xAl_{100-x} (32<x<90) elemental blends[168]. Subsequent efforts[169-173] have confirmed the previous results of solid state synthesis in the Ni-Al system. Though a considerable extension of phase fields in the Ni_3Al, NiAl and even in the line compound $NiAl_3$ have been observed under intensive milling conditions[169,171], Ni_2Al_3 and Ni_5Al_3 phases were found metastable under similar conditions[169]. It is of interest to note that, in a marked contrast to the gradual temperature rise (~348K) during MA of Ni-aluminides in laboratory ball mill under air[168], formation of NiAl in Spex 8000 mill under Ar atmosphere[170] was accompanied by an exothermic reaction within a short duration of milling following an interruption after 2*h* of continuous milling. A similar observation has also been reported recently[174] on low energy ball milling of $Ni_{50}Al_{50}$ as well. Recent studies by Liu *et al.*,[175] have revealed a delayed initiation of the exothermic NiAl phase formation reaction on addition of ternary alloying elements such as Ti and Fe as indicated in Fig. 11. The occurrence of explosive reaction was also observed on opening the vial following milling[174]. This suggests the possible role of energy liberated during oxidation of Al in promoting the Ni-Al reaction. On the other hand, the absence of catastrophic reaction when milled in air[168] could be attributed to the continuous oxidation of the

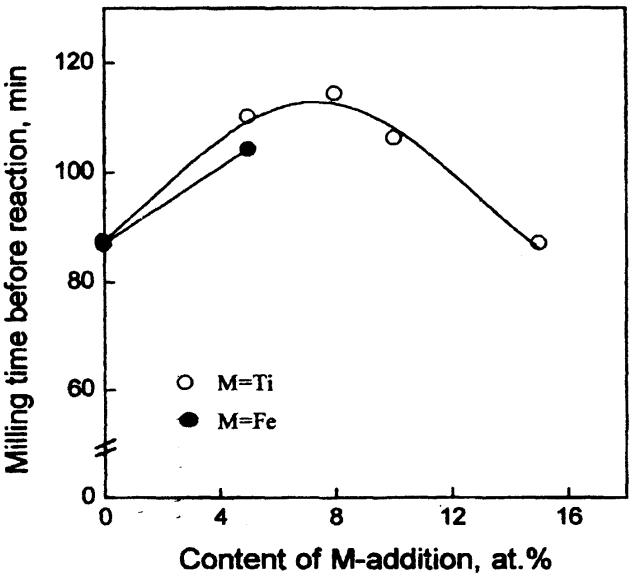

Fig. 11 Influence of ternary additions on the initiation of exothermic NiAl phase formation reaction[175]

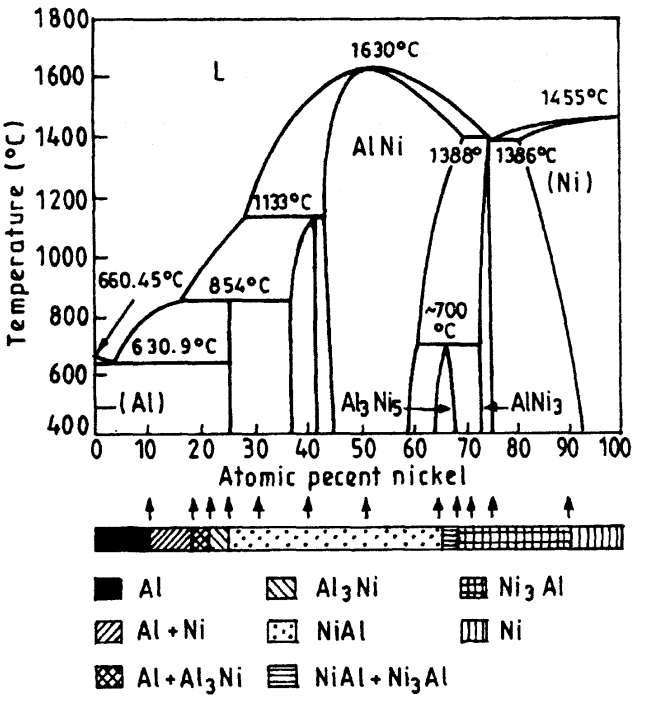

Fig. 12 Extended phase fields of Ni-aluminides under MA

elements and the slow diffusion between the oxide coated ingredients, which results in reduced reaction kinetics. Pabi and Murty[176] have observed wide phase fields for the Ni aluminides (Fig. 12) in the nanocrystalline state and could explain the large extension in the NiAl phase field in the nanocrystalline state based on thermodynamic considerations (Fig. 13)[141].

Ti-Aluminides: Investigations on Ti-Al intermetallics have revealed stiff resistance to alloying during MA. For example, prolonged milling for 100h in Fritsch P-5 planetary mill at a BPR of 10 has failed to produce Ti-Al compounds[177]. The formation of Ti-Al intermetallics could be achieved on adopting a two stage process involving MA and subsequent annealing[178]. This is evidenced by the MA efforts for the synthesis of TiAl and $TiAl_3$, which required annealing of the ball milled ingredients at 873 and 813K respectively[179]. Several other reports on the production of Ti-Al intermetallics such as $TiAl_3$, Ti_2Al_3, TiAl and Ti_3Al through a 'mechanically activated annealing process' involving intense ball milling followed by annealing process are also available[180,181]. It is, however, quite obvious that the annealing temperatures would vary considerably depending on the final crystallite sizes which dictates the diffusion distance. On the other hand, there also exist some reports of direct synthesis of Ti-Al intermetallics by MA. For example, the formation

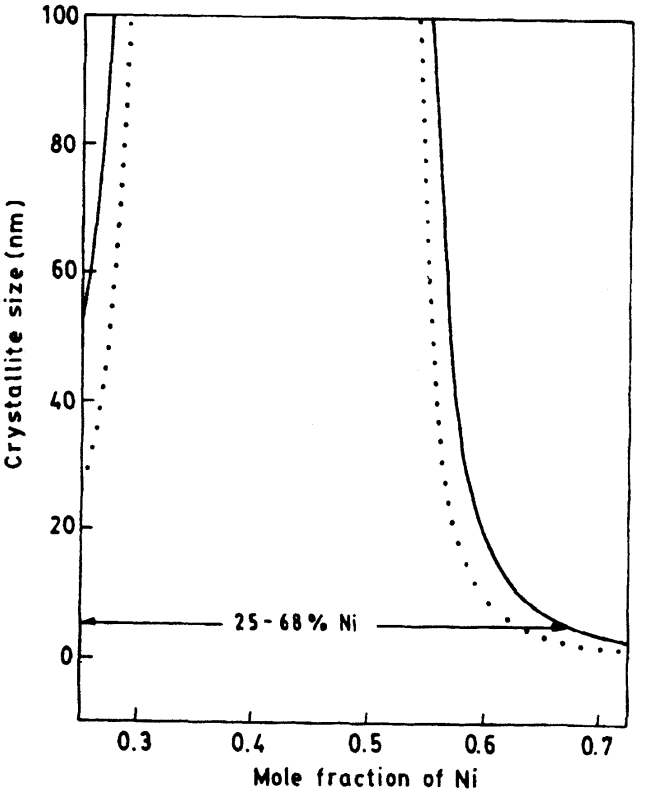

Fig. 13 Role of crystallite size on the thermodynamic stability of NiAl over an extended phase field

of TiAl and Ti_3Al has been reported during MA of $Ti_{40}Al_{60}$ and $Ti_{50}Al_{50}$ elemental blends[182]. Moreover, investigations by Park *et al.*,[183] have shown successful synthesis of TiAl and Ti_2Al through direct MA in vibratory mill in stainless steel grinding media with 12.7 and 19.1mm diameter grinding balls. However, the extent of Fe-contamination and its possible role in triggering such a reaction during MA remain to be looked into. Suryanarayana *et al.*,[184] could synthesize TiAl by MA of $TiAl_3$ and TiH_2.

Fe-Aluminides: $FeAl_3$ formation during MA of $Fe_{20}Al_{80}$ and $Fe_{25}Al_{75}$ blends in Fritsch P-5 planetary ball mill is quite well documented[185,186]. Interestingly, the initiation of $FeAl_3$ formation occurred within 40*h* in the $Fe_{25}Al_{75}$ blend as against 65*h* in $Fe_{20}Al_{80}$. Such a delayed synthesis of $FeAl_3$ in $Fe_{20}Al_{80}$ is quite explicable due to the off-stoichiometric composition. No intermetallic compound has been detected in Fe-87.5at.%Al blend even after 80*h* of MA[185,186]. Subsequent annealing at 773K, however, resulted in $FeAl_3$ phase. The formation of such non-stoichiometric $FeAl_3$ may be an indication of an extended $FeAl_3$ phase field, though, any possible Al loss due to oxidation may also be responsible for such observation. MA of Fe-rich composition, *e.g.*, Fe-25at.%Al, which incidentally lies in the Fe_3Al phase field, has been found to produce FeAl instead[187]. Subsequent annealing, on the other hand, has led to B2- Fe_3Al instead of the usual DO_3 structure. The formation of FeAl during MA in preference to $AlFe_3$ has been attributed to its more negative Hf (–31.8kJ/mol) when compared to that of Fe_3Al (–18kJ/mol). The formation of metastable Fe_2Al_5 through MA has also been demonstrated[188] within 0.5*h* in Spex 8000 mill at a BPR of 6, which finally transformed to a more stable FeAl on MA for 5*h*.

Other Aluminides: Apart from the above mentioned Ni, Ti and Fe aluminides, MA has demonstrated its ability in the synthesis of several other aluminides including ternary aluminides. Some of these aluminides includes Cu-Al, Nb-Al, Mo-Al, Zr-Al, Al-Ni-Fe, etc. A list nanocrystalline aluminides synthesized by MA is presented in Table VII.

3.3.2 Silicides

The MA of silicides has gained significant interest in recent years[206], particularly because of their potential applications as structural materials in the field of microelectronics and electrical technology.

Ni-Silicides: The initial efforts by Radlinski and Calka[207] on the synthesis of Ni-Si intermetallics through MA of an equiatomic blend of Ni-Si failed to produce the desired product even after prolonged milling for 1000*h*. However, subsequent annealing treatment at 973K for a period of 1*h* did result in the formation of NiSi. On the other hand, studies on MA of $Ni_{100-x}Si_x$ (x=25, 28, 33, 40 and 50) in Fritsch P-5 at a very high vial speed of 642rpm revealed crystalline phase formation in Ni_3Si, Ni_3Si_2 and NiSi compositions and an amorphous phase in Ni_5Si_2, Ni_2Si compositions[208]. Recently, Datta *et al.*[209], studied the MA characteristics of the entire range of composition in Ni-Si system. They have observed that only congruent melting silicides form in the nanocrystalline state and the formation of non-congruent silicides is suppressed even at their

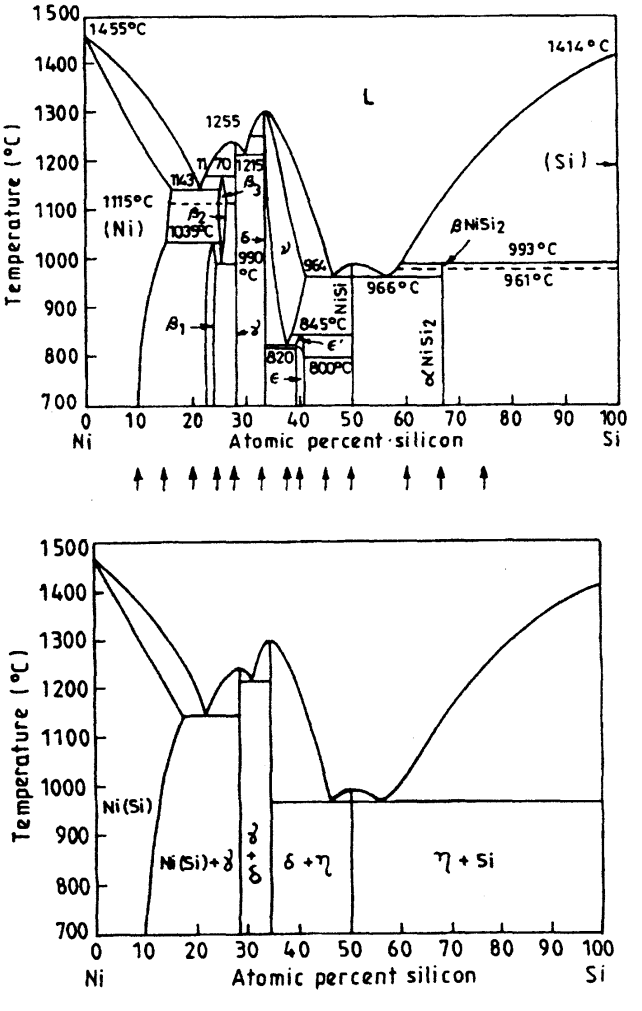

Fig. 14 (a) Equilibrium Ni-Si phase diagram indicating compositions subjected to MA and (b) metastable phase diagram at nanocrystalline state

Table VII
Nanocrystalline Aluminides Synthesized by MA

Phase	Structure	ΔH_f (kJ/mol)[187]	Synthesis Route	Reference
AlCo	B2	-43	MA	190
Al_4Cu_9	$D8_2$	-8	MA	191
Al_3Hf	$L1_2$	-51	MA	192
Al_3Mg_2	Fcc	-3	MA	193
$Al_{12}Mg_{17}$	A12	-3	MA	193
Al_6Mn	Orthorh	-15	MA	194
AlMn	B2	-43	MA	194
$Al_{12}Mo$	Bcc	-5	MA+HT	195
Al_5Mo	hex	-10	MA+HT	195
Al_4Mo	Monocl	-13	MA+HT	195
Al_8Mo_3	Monocl	-17	MA+HT	195
$AlMo_3$	Monocl	-15	MA+HT	195
Al_3Nb	DO_{22}	-29	MA	196,197
$AlNb_2$	$D8_2$	-36	MA+HT	197
$AlNb_3$	A15	-28	MA+HT	198-200
AlZr	Orthorh	-83	MA	197
Al_3Zr_2	Orthorh	-80	MA	197
Al-49Ni-2Cr	B2		MA	201
Al-46Ni-8Cr	B2		MA	201
Al-42Ni-16Cr	B2		MA	201
Al-40Ni-20Cr	A2		MA	201
Al-Ni-Fe	B2		MA	175,202
Al-49Ni-2Fe	B2		MA	201
Al-46Ni-8Fe	B2		MA	201
Al-42Ni-16Fe	B2		MA	201
Al-40Ni-20Fe	A2		MA	201
Al-Ni-Ti	B2		MA	171,175,203
Al-25Zr-3Fe	$L1_2$		MA	197
Al-25Zr-8Fe	$L1_2$		MA	204
Al-25Zr-8Ni	$L1_2$		MA	204
Ti-24Al-11Nb	B2		MA	197,205
Ti-25Al-25Nb	B2		MA	205
Ti-28 5Al-23 9Nb	B2		MA	197
Ti-37 5Al-12 5Nb	B2		MA	197

HT : Heat treatment

equilibrium compositions. Thus, in the nanocrystalline state the phase fields of silicides are given by the metastable phase diagram in comparison to the stable phase diagram as shown in Fig. 14(a) and (b).

Fe-Silicides: MA efforts with elemental $Fe_{33}Si_{67}$ blend[210] have shown the formation of a mixture of low temperature-tetragonal α–$FeSi_2$, high temperature-orthorhombic β–$FeSi_2$ and the cubic FeSi phases. MA studies on $Fe_{100-x}Si_x$ (x=5, 25, 37.5 and 50) in Fritsch P-7 at a BPR of 12 have revealed the formation of FeSi, Fe_2Si, Fe_5Si_3 and $FeSi_2$ respectively[211]. However, MA of Fe-6.5wt.%Si has shown the formation of a solid solution[212]. In fact, extremely high intensity MA[213] has demonstrated the formation of Fe-Si solid solution over an extended phase field up to Fe-37.5wt.%Si. On the other hand, MA studies in the Si-rich composition regimes in horizontal ball mill[214] have revealed the formation of β–$FeSi_2$ phase for Si>70at.% and ε+β–$FeSi_2$ at 50at.%<Si<70at.%.

Ti-Silicides: In the initial studies on MA of Ti-Si system by Veltl *et al.*[215] in planetary ball mill, no intermetallic formation in the intermediate stages of milling have been detected possibly due to fast amorphization reaction in the high energy milling. However, the generation of TiSi intermetallic phase prior to amorphization during MA has been observed within 4h in Vibro mill at higher BPR[216]. MA results reported by Oehring and Bormann[217] and Park *et al.*,[218] demonstrate the formation of crystalline Ti_5Si_3, which remained stable even on prolonged milling. Such a high stability of Ti_5Si_3 against amorphization during milling is in conformity with its large negative free energy of formation (~-71kJ/mol at 673K). Recent studies on MA of elemental blends of compositions

$Ti_{33}Si_{67}$ and $Ti_{42}Si_{58}$ have shown the formation of crystalline Ti_5Si_3 and Ti_5Si_4 embedded in an amorphous matrix after 60h of milling in Vibro mill[219]. $TiSi_2$ and TiSi phases were also detected in the preliminary stages of milling (4h) in this study, which paved way to the more stable phases with the progress of milling.

Mo-Silicides: Most of the research work on MA of Mo-silicides has been primarily focused on the Mo-disilicide ($MoSi_2$), which is a well-known refractory intermetallic (melting point=2323K) with considerable technological importance. Successful synthesis of $MoSi_2$ by MA has been reported by Schwarz *et al.*,[220] in Spex 8000 mill within 70h. More recently, nanocrystalline $MoSi_2$ has been synthesized by MA of $Mo_{33}Si_{67}$ in planetary ball mill (Fritsch P-5) at a disc speed of 280rpm[221]. Interestingly, both the low temperature as well as the high temperature phases *viz.*, α and β-$MoSi_2$ occurred during MA, with the extent of β phase increasing with milling time. Lee *et al.*[222], have reported that the formation of $MoSi_2$ during MA is quite sensitive to the type of mill used. While both α and β-$MoSi_2$ could be obtained by MA in Spex mill, MA in planetary mill could not yield the silicide even after subsequent annealing treatment. In a significant report, Liu and Magini[223] have shown that high energy ball milling results in a self propagating high temperature synthesis (SHS) reaction leading to stable α-$MoSi_2$, while low energy milling leads to metastable β–$MoSi_2$ without any such reaction.

Other Silicides: The development of silicides other than the Ni, Fe, Ti and Mo-silicides through MA has evoked only limited interest so that only a handful of such reports is available. Some of these have been on the Pd-silicides. It is interesting that while high energy ball milling[224] resulted in the formation of the line compound Pd_3Si along with an amorphous phase from a mixture of composition Pd-16-23at.%Si elemental blend, low energy milling[225] of Pd-17at.%Si led only to an amorphous phase. The direct synthesis of Pd_2Si has been reported on MA of Pd-Si blends with Si>33at.% while at Si>50at.%, initial product of Pd_2Si is destabilized on prolonged milling and gradually transformed to the high temperature PdSi phase[226]. Nb_5Si_3 and Ta_5Si_3 compounds have also been synthesized through MA of elemental blends[227]. Lou *et al.*,[228] have shown that milling without interruption leads to the abrupt formation of $NbSi_2$, while regular interruption results in its gradual formation. Unlike in $MoSi_2$ where prolonged milling resulted in the transformation of the low temperature phase (α) to the high temperature phase (β), the progress of MA of Nb_5Si_3 in Spex mill[229] led to the formation of more of the room temperature phase (α) at the expense of the high temperature phase (β).

3.3.3 *Other Intermetallics*

Though the aluminides and silicides have stolen the lime light in the field of research on MA of intermetallics, several other intermetallics deserve notable mention due to fundamental aspects as well as technological importance. The formation of various compounds in the Cu-Zn system *viz.*, β-CuZn, γ-Cu_5Zn_8 and ε phases, through MA has been extensively studied over the last decade[80,230,231]. Studies have shown that a sequence of phase formation is maintained during milling of elemental Cu-Zn blends in Fritsch P-5, wherein, the Zn-rich phases e.g. ε, and/or γ were always the first to form[80]. This is attributed to the much higher diffusivity of Cu in Zn than *vice versa*[80]. The progress of milling has shown the gradual formation of the Cu-rich phases through a continuous diffusive mechanism. The synthesis of superconducting intermetallics by MA e.g., Nb_3Sn has also been successful[232], while efforts on MA of superconducting Nb-Ge system has led to successful production of a number of phases *viz.*, Nb_3Ge, Nb_5Ge and $NbGe_2$ depending on the composition of the starting blend[233,234]. A list of non-aluminide and non-silicide intermetallics produced by MA is presented in Table VIII.

A number of metastable intermetallics have been obtained during MA in the nanocrystalline state. A bcc phase has been obtained at an elemental composition ratio for Nb_3Al instead of the equilibrium A15 compound[120] and a hcp phase at Ti_3Al, where the equilibrium structure is DO_{19}[177]. Similarly, $TiSi_2$ phase with metastable C49 structure has been obtained both by MM of equilibrium C54 structure and by MA of Ti and Si[249]. Formation of hexagonal C14 phase, metastable at room temperature has been obtained in stead of stable C15 cubic Cr_2Nb during MA[250].

3.4 *Nanocomposites*

In recent years, there have been considerable efforts to produce *in-situ* nanocomposites by MA. Zhu *et al.*,[251] have synthesized Pb-Al and Fe-Cu nanocomposites by MA. In a similar attempt,

Table VIII

Nanocrystalline Intermetallics other than Aluminides and Silicides Synthesized by MA

Phase	Structure	ΔH_f (kJ/mol)[189]	Synthesis Route	Reference
Co_3C	hex	+6	MA	235,236
Cr_7C_3	hex	-13	MA+HT	237,238
Cr_3C_2	orthorh	-16	MA+HT	237,238
Cr_2Nb	C15	-10	MA	239
β-CuZn	B2	-8	MA	80,230,231
γ-Cu_5Zn_8	$D8_2$	-4	MA	80,230
ε-$CuZn_4$	hex.	-2	MA	80,230
Fe_3C	orthorh.	+25	MA	236
$FeSn_2$	C16	-1	MA	240
Fe_3Sn_2	monocl	-2	MA+HT	240
FeSn	B35	-2	MA+HT	240
Fe_3Sn	DO_{19}	-2	MA	241
Fe_3Si	DO_3	-21	MA	241
FeTi	B2	-25	MA	242
Fe_3Zn	$D8_2$	-2	MA	241
Mg_2Ge	C1	-115	MA	243
Mg_2Ni	hex	-52	MA+HT	244
Mg_2Si	C1	-79	MA	243
Mg_2Sn	C1	-80	MA	243
Nb_3Ge	A15	-28	MA	233,234
Nb_5Ge	orthorh	-19	MA	234
$NbGe_2$	C40	-29	MA	234
Nb_3Sn	A15	-16	MA	232
Ni_3B	cubic	-21	MA	245
Ni_3C	cubic	+7	MA	235,236
Ni_3Sn_2	hex	-24	MA	240
TiB_2	hex	-74	MA	207
TiC	$L1_2$	-77	MA	246-248
TiNi	B2	-52	MA	248

Provenzano and Holtz[252] have shown the formation of Ni-Ag and Cu-Nb nanocomposites by MA. Du *et al.*,[253] have produced Al-BN composites by high energy ball milling. In an interesting report, Naser *et al.*[254], have showed that no grain growth occurs in the matrix close to its melting point when Cu and Mg are reinforced with nanocrystalline Al_2O_3 by mechanical alloying. Wu *et al.*,[255] have reported the formation of nanocrystalline TiC in an amorphous Ti-Al matrix by MA. A solid state reaction leading to the formation of AlN and AlB_2 was reported by them during further processing of these nanocomposites. TiAl-Ti_5Si_3 nanocomposites have been reported by Liu *et al.*,[256] by MA followed by thermal treatment. They attribute the formation of these nanocomposites to the crystallization of amorphous phase obtained by MA in Ti-Al-Si system. These nanocrystalline compounds appear to be quite stable and no significant coarsening was observed even after heat treatment for 1*h* at 1273K. Similar nanocomposites have been obtained by Senkov *et al.*,[257] by MA and subsequent heat treatment of a mixture of TiH_2 and Al-Si alloy powders. $NbAl_3$-NbC nanocomposites have been

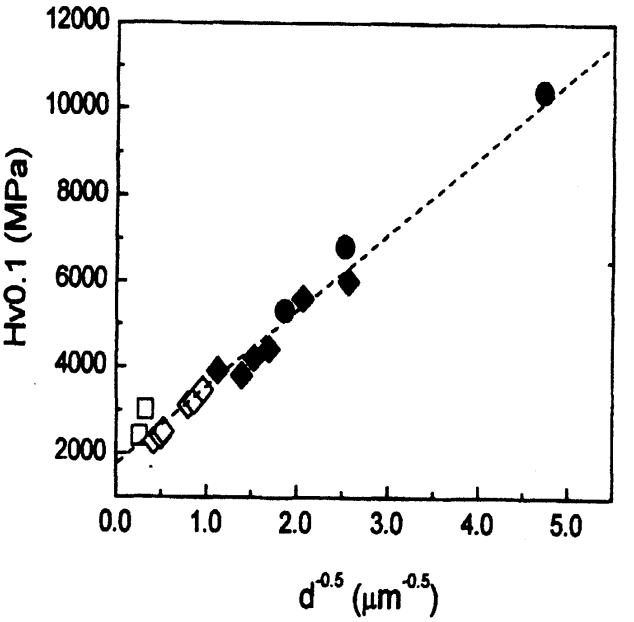

Fig.15 Change in the microhardness of Ti-Al alloys with $d^{-1/2}$(●), mechanically alloyed Ti-46at %Al-5at %Si and Ti-20at %Al-17at %Si-9 5at %Nb; (♦), mechanically alloyed binary Ti-Al; (↓), conventional powder-processed material; (⌟), ingot material of similar composition[260]

obtained by MA of Al and Nb powders[258]. Interestingly, NbC in this case appears to have formed by the reaction of Nb with the methanol medium in which the milling was performed. Manna *et al.*,[259], have recently synthesized nanocomposites of Cu-$NbAl_3$ by the codeposition of nanocrystalline $NbAl_3$ during the electrodeposition of Cu. Pfullmann *et al.*,[260] have mechanically alloyed TiAl base alloys with Si to synthesize nanocomposites with Ti_5Si_3 dispersions in TiAl and Ti_3Al and found significant improvement in microhardness in the nanocrystalline state (Fig.15).

4 Mechanism of Nanocrystalline Phase Formation during MA

The phase formation processes to a great extent are influenced by the chemical driving force provided by the free energy/enthalpy difference. In case of nanocrystalline materials, the contribution of interfacial energy term becomes comparable with the chemical free energy term, and hence has a decisive role in dictating the stability of equilibrium phases in the milled product. For instance, precipitation of second phase particles in nanocrystalline supersaturated solid solution is going to be difficult due to further increase in interfacial areas. For this reason, reactions like discontinuous precipitation or peritectoid transformations are expected to be suppressed in nanocrystalline alloys. The large density of dislocations generated in the as milled products under heavy cold work involved during MA can also contribute to the enhanced diffusivity values and thereby significantly influence the alloying mechanism[261]. The studies on ball milling induced alloying has broadly led to three major type of mechanisms as discussed below:

(a) Continuous Diffusion (CD) of Reacting Species

The mechanism is characterized by a continuous change in the lattice parameter of the solvent with the progress of milling at the expense of the depleting solute content. Zbiral *et al.*,[262] have proposed two different mechanisms (I and II) occurring via CD mode. In mechanism I, for a lower solubility of A in B compared to B in A in the A-B system, alloying is achieved by diffusion of the B into A. Such mechanism has been suggested to be relevant to binary model systems e.g., Ni+Al, Ni+Ti, Ni+Cr, Ni+Mo, Ni+W. While mechanism II has been proposed to operate in systems with good mutual solubilities e.g., Ni+Cu, Ni+Ta and Ni+Zr. Fig.16 illustrate the two alloying mechanisms and indicate the direction of diffusion and alloy growth.

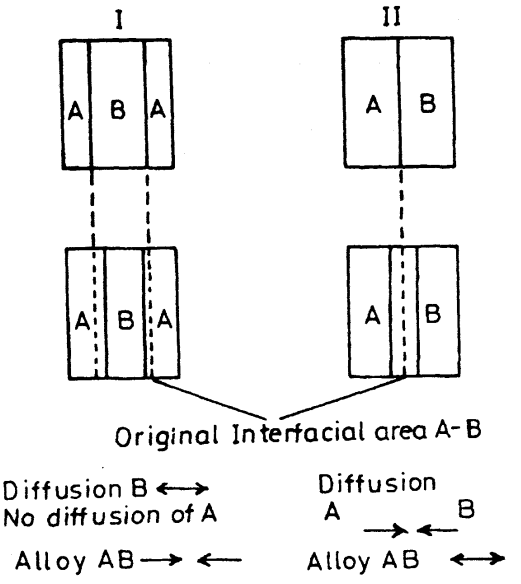

Fig. 16 Alloying mechanism by continuous diffusive mode[262]

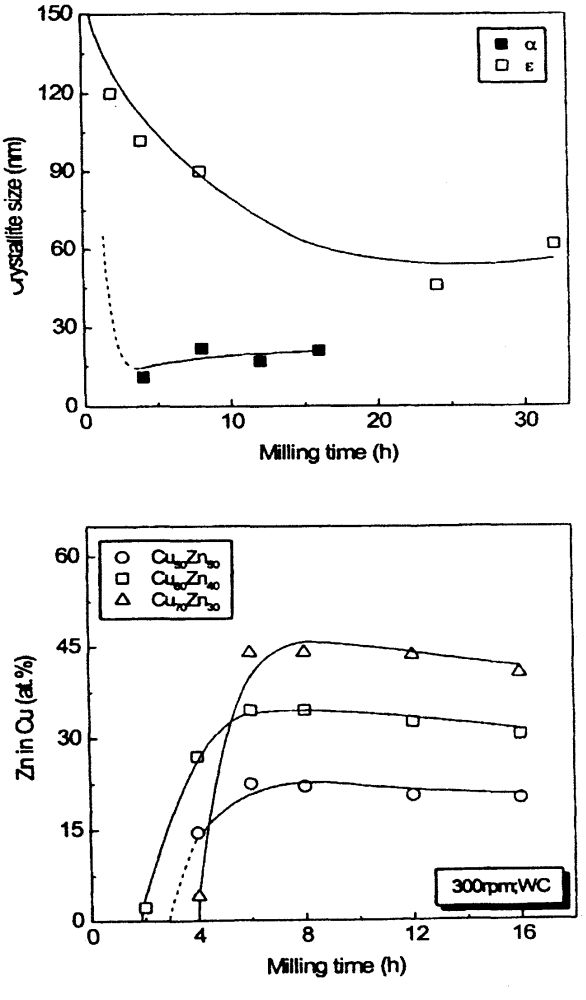

Fig. 17(a) Changes in the crystallite size of α and ϵ and (b) variation in the solubility of Zn in Cu during MA of different Cu-Zn blends

Recently, the mechanism of mixing has also been analyzed in Cu-Zn model system[80], which is characterized by ΔH_f ~ -6 to -9kJmol^{-1}. As evident from Fig.17a, the formation of α and ε-phases occur with the reduction in crystallite sizes of (Cu). A concomitant increase in the amount of Zn dissolved in Cu at the initial stages of milling is also estimated (Fig.17b), which indicates fast diffusion of the species at nano-grain sizes. Interestingly, alloying was found to initiate by the diffusion of Cu into Zn so that even at a Cu-rich composition in equilibrium α phase field, the Zn-rich phases *viz.* η or ε were first to form. These Zn-rich phases were however metastable, and paved way for the more stable phase(s) at the particular composition. The above behaviour may be easily understood if one looks into the diffusivities of Cu and Zn in each other (extrapolated at the probable milling temperature of ~473K from high temperature data[263]) which indicate nearly eight order of magnitude higher $D_{Cu\ in\ Zn}$ (2.99×10^{-14}cm^2/s) when compared to $D_{Zn\ in\ Cu}$ (8.21×10^{-23}cm^2/s). Similar mixing behaviour has also been observed in Cu-Ni system as reported by Pabi *et al.*[264]

(b) Self-Sustaining Reaction (SR)

Though, in real sense SR mechanism is more a reaction synthesis mechanism rather than a MA mechanism, it deserves attention because of the indications in several reports that similar process possibly play the crucial role in the overall alloying behaviour by increasing the milling temperature drastically, which in turn promotes the desired reaction. For example, the synthesis of Ni-Al intermetallic from Ni-Al blend has been reported to be associated with an exothermic reaction due to oxidation during milling which supports the reaction leading to generation of phase(s)[170,265]. The role of crystallite size and lattice strain, however, has been overlooked and warrants critical assessment. In an effort to develop a well defined criteria for self sustaining reaction it has been suggested[60] that for the reaction to occur the required diffusion distance, must decrease relatively more rapidly than the accomplished diffusion distance (X_D) increases (Fig.18).

(c) *Discontinuous Additive (DA) Mixing*

The mechanism is characterized by the typical behaviour of the crystallite size refinement whereby the crystallite size of the product at the onset of its

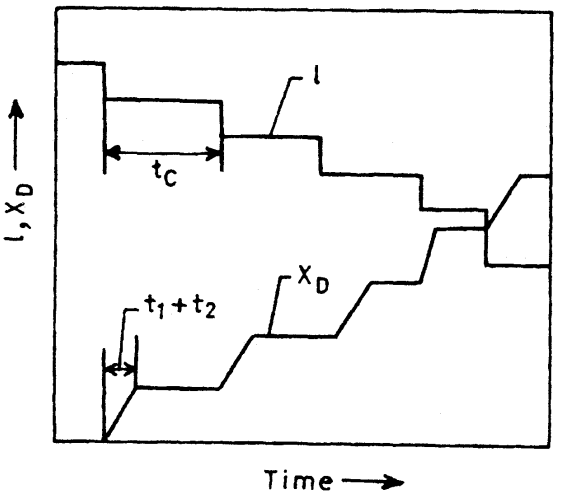

Fig. 18 Schematic of a reaction process where the phase evolution occurs at a time, t, when the required diffusion distances (l) as well as the accomplished diffusion length (X_D) converges[60]

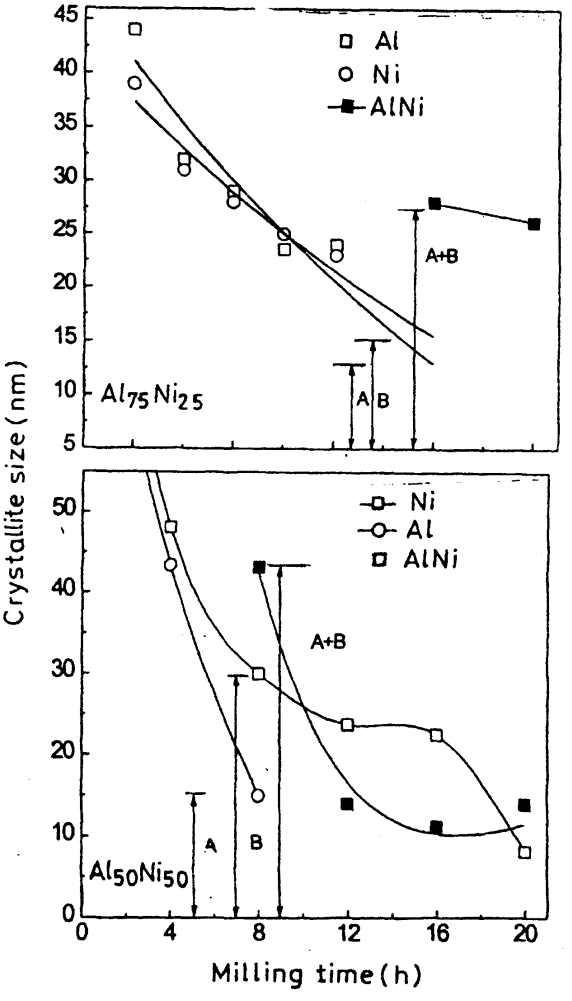

Fig. 19 Discontinuous additive mixing during NiAl formation from (a) $Ni_{25}Al_{75}$ and (b) $Ni_{50}Al_{50}$ blend compositions by MA

formation is equal to the sum of the individual crystallite size of the constituents[264]. It may be noted that the mixing behaviour during MA of binary Ni-Al blends as analyzed in various prototype compositions *viz.* $Ni_{21}Al_{79}$, $Ni_{25}Al_{75}$, and $Ni_{50}Al_{50}$ have revealed similar behaviour. Interestingly, the formation of ordered NiAl from $Ni_{25}Al_{75}$ and $Ni_{50}Al_{50}$ blends initiates when the crystallite sizes of the ingredients, Ni and Al, at the onset of the reaction shows an additive relation when compared to that of the product, NiAl (Fig.19(a) and (b)). Furthermore, the critical crystallite size of the constituents, at which the DA mixing is triggered, depends on the composition and it is largest at the stoichiometric composition (*i.e.*, $Ni_{50}Al_{50}$) apparently for maximum available driving force[264]. This does not fit to the conventional continuous diffusive mixing mechanism. It may be recalled that earlier reports[170,265] have indicated the association of a sudden exothermic reaction in the vial during the synthesis of NiAl from a stoichiometric blend composition, which is suggestive of reactive mixing as stated in the previous section. However, in reactive mixing the reaction front usually propagates in unpredictable direction and is, therefore, unlikely to show additive rule as observed by Pabi *et al.*[264] In addition, as milling in these studies were performed under liquid (toluene) bath, high temperature build-up at the collision point is unlikely. The temperature estimates from earlier studies 94 points to a modest rise in temperature (~ 473-573K). It is noteworthy to mention in this connexion that studies on external heating of Ni-Al powder compacts in atomic volume of 1:3 at a heating rate of 8.33 x 10^{-2}K/s shows the initiation of a self propagating high temperature reaction (SHS) at ~823K[266]. While, studies on Ni-Al foils at overall compositions between Ni-25 to 75at.%Al have indicated that the initiation of SHS required a temperature of greater than or equal to the melting point of Ni[267]. Thus, the discontinuous additive mode of mixing is quite unique, which may, however, be looked upon as a low temperature version of reaction synthesis.

4.1 Factors Controlling the Mixing Mechanisms

It may be noted that the mechanically induced energy may even supersede any thermodynamic or kinetic barrier to instigate reaction in otherwise immiscible systems. The difference in the alloying behaviour in various systems may be, therefore, evaluated within a framework delineated by distinct ranges of enthalpy of formation/mixing. On the other hand, recent investigations also point to the possible influence of the ordered structure of the mechanically alloyed products in determining the mode of alloying. These aspects need greater attention for an in-depth understanding of the underlying fundamentals, which has not been attempted so far.

4.1.1 Influence of ΔH_{mix}

I $\Delta H_{mix} < 0$

The above condition thermodynamically favours alloy formation. However, the occurrence of the reaction during MA from elemental blends is likely to be decided by the kinetic factors. The system has to surmount the activation energy barrier by the mechanical energy impounded into the ultra-fine-crystal ensembles and once it crosses this barrier the reaction is sustained by an enhanced downhill diffusion. Though, there exist no distinct criteria defining the alloying mechanism involved during MA, three different modes have been reported to operate in several systems *viz.* a continuous diffusion induced transformation, a self sustaining reaction assisted by some exothermic process accompanying ball milling and also the discontinuous additive mixing mode observed in aluminides as discussed in previous section.

II $\Delta H_{mix} > 0$

The positive heat of mixing in system implies lack of chemical driving force for alloying and as such, the formation of intermediate phases or solid solution is thermodynamically not feasible under equilibrium conditions. The mechanism underlying the solid solution formation in systems with positive ΔH_{mix} under the non-equilibrium MA processing have been found to be of CD type. The alloying process in these systems has opened up several possibilities based on the source of driving force as mentioned below. It may be noted that all these mechanisms suggested for systems with positive heat of mixing could well be applicable for systems showing negative enthalpy of mixing.

(a) Energy Stored in Grain Boundary

The large grain boundary energy has been correlated to the occurrence of solid state alloying based on the observation that reaction proceeds as the crystallite sizes of elemental constituents drops down to nanometric level[154]. Substantial amount of enthalpy is expected to be stored in the nanocrystalline metal due to large grain boundary area[31].

(b) Oxygen Induced Mixing

The possible reduction in the enthalpy of mixing of systems by the dissolution of oxygen has also been suggested to induce alloy formation in liquid immiscible systems e.g., Cu-Ta and Cu-W, both of which have tendency to form amorphous phases on milling[39]. This has been supported by the reported reduction in the heat of transformation of amorphous $Cu_{30}Ta_{70}$ to elemental state of only 3-11kJ/g atom[153,267] from the expected value of ~20kJ/g atom. However, no such change in the enthalpy of mixing has been reported in Cu-Co system[148] even for higher amounts of oxygen.

(c) Capillary Pressure Mechanism

The mechanism suggested by Yavari *et al.*,[143] for composites of Cu with Fe or other high-melting bcc metals, having positive ΔH_{mix}, considers fracturing of the composite on deformation, with the formation of fragments of small tip radii. Such structure leads to capillary pressure build-up at the small tips, which in turn forces, the atoms of the fragments to dissolve. Yavari *et al.*,[143] has further shown that for an incoherent Cu/Fe interface enthalpy of 1.4J/m2, dissolution of Fe atom in Cu occurs for a tip diameter ≤14nm.

(d) Dislocation Assisted Alloying

High dislocation density may also contribute to a substantial increase in the mutual solubility in systems with positive ΔH_{mix}[144]. This is due to change in the chemical potential of the solute atoms in the strain field of an edge dislocation. Such mechanism has been extended to account for the metastable solid solubility in Cu-Fe system under ball milling[144].

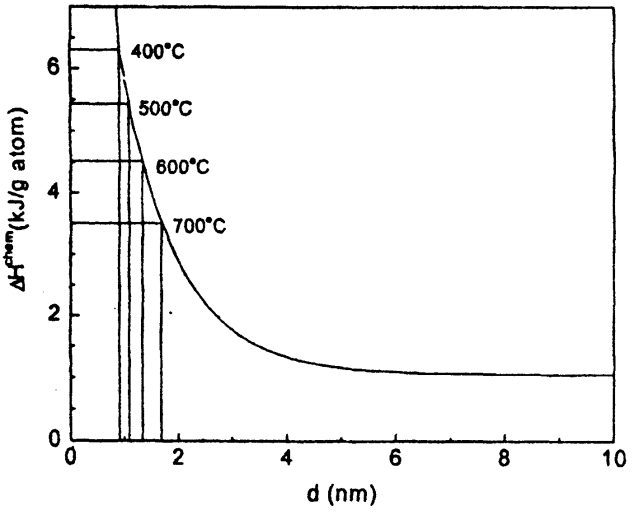

Fig. 20 Chemical contribution of interface enthalpy with the refinement of microstructure[158]

(e) Influence of Coherent Interface

Apart from the excess structural enthalpy of the system on account of the grain refinement during ball milling, coherent interface formation in systems, *e.g.*, Cu-Co (between Cu and Co regions) has been considered to play significantly in the solid solution formation[158]. It has been argued that the formation of such coherent interface between Cu and Co regions does not change the crystallite size so that the thickness of the elemental components in the final state may be much smaller than their crystallite sizes, enhancing the chemical contribution of the interface. The critical size, d_C, below which the chemical contribution of the Cu-Co interface enthalpy exceeds the free energy of the solid solution, has been calculated from simple energy relations, neglecting the small entropy contribution to the free energy of interface. The enhancement in the chemical contribution of interface enthalpy with the refinement of microstructure has been shown in Fig.20 for different sizes of Cu and Co regions. Considering an enthalpy of $0.3Jm^{-2}$ for the coherent Cu/Co interface for d_C ~1nm, the ΔH_{chem} for $Cu_{50}Co_{50}$ composite raises above 6kJ/g atom which is sufficient to allow for a phase transformation of the composite into solid solution provided the interface temperature reaches ~673K during ball milling operation.

4.1.2 Influence of Ordering Characteristics

The various mechanisms controlling the phase formation reactions during MA have been investigated in Cu-Al, Nb-Al, Ni-Al and Fe-Al systems having $\Delta H_f << 0$. It has been attempted to generalize the theory propounded for these systems by comparing with alloying mode in Cu-Zn possessing less negative Hf and Cu-Ni with $\Delta H_f > 0$. Table IX presents the various alloying mechanisms operating in these systems during MA. As it evolves from the above table (Table IX)[268], there exists contrasting mode of mixing in the ordered products *viz.* $NiAl_3$ and NiAl on one hand and the disordered products e.g., Ni_3Al and FeAl on the other. The Table reflects the possible role played by the structural order in the product phase in determining the synthesis mechanism. This is elucidated by the influence of a highly disordered

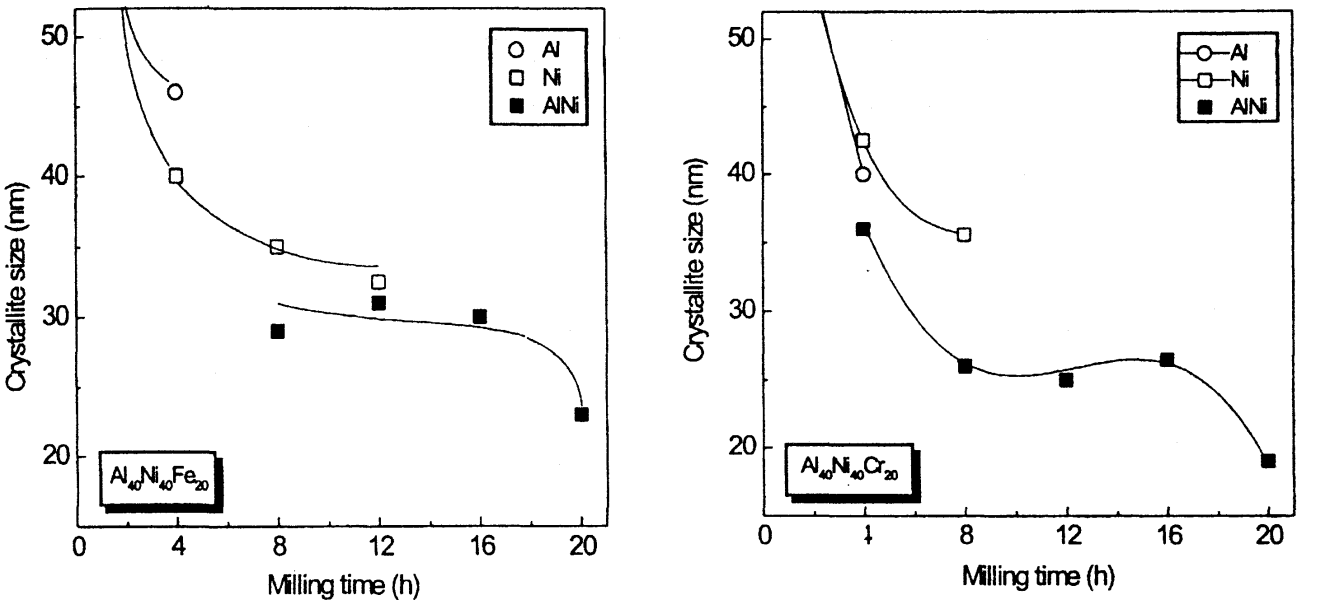

Fig. 21 Crystallite size variation with milling time in the formation of NiAl during MA of (a) $Ni_{40}Al_{40}Fe_{20}$ and (b) $Ni_{40}Al_{40}Cr_{20}$ blends

Table IX

Alloying Mechanism in Different System during MA[26]

System	Composition	Product phase	C S (nm)	Product nature	ΔH_f (kJ/mol)	Alloying mechanism
Cu-Ni	$Cu_{50}Ni_{50}$	Cu(Ni)	20	DO	2	CD
Cu-Zn	Cu-15 to 50at %Zn	α	20	DO	-9	CD
Cu-Al	$Cu_{80}Al_{20}$	Cu(Al)	10	DO	-8	CD
Fe-Al	Fe-25 to 50at %Al	FeAl	15	DO	-31	CD
Ni-Al	Ni-21at %Al	$NiAl_3$	20	ORD	-39	DA
	$Ni_{50}Al_{50}$	NiAl	10	ORD	-72	DA
	$Ni_{75}Al_{25}$	Ni_3Al	30	DO	-42	CD
Ni-Al-Fe/Cr	$Ni_{40}Al_{40}Fe_{20}$	NiAl	25	DO	–	CD
	$Ni_{40}Al_{40}Cr_{20}$	NiAl	20	DO	–	CD
Nb-Al	$Nb_{25}Al_{75}$	Nb_3Al	9	ORD	–20	CD

C.S. =crystallite size after 20h of MA; ORD=ordered; DO=disordered (S≤0.3); CD=continuous diffusive mixing; DA=discontinuous additive mixing;

ball milled NiAl, caused by Fe or Cr additions as described in ref. [47], on the mixing phenomenon (see ref. [28]). Interestingly, the crystallite sizes at the onset of the formation of the highly disordered NiAl in NiAl(+Fe/Cr) blends do not demonstrate the usual additive relation as evident from Fig.21(a) and (b). However, a gradual shift in the lattice parameter of Ni caused by the gradual consumption of Al with progress of milling is observed (Fig.22), that evidences a continuous diffusive mixing mode in the disordered NiAl. It may be noted that though Fig. 22 reports the variation of Ni peak in $Ni_{40}Al_{40}Cr_{20}$ only up to 8*h* its presence was evident till 16h. However, it was difficult to ascertain the lattice parameter as well as crystallite size because of its highly diffused nature. Furthermore, it may be mentioned that a considerably higher diffusivity values are usually

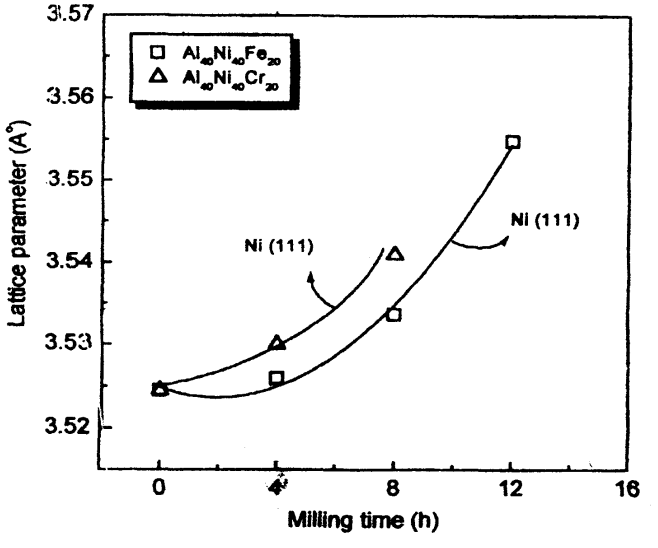

Fig.22 Shift in lattice parameter of Ni during MA of $Ni_{40}Al_{40}Fe_{20}$ and $Ni_{40}Al_{40}Cr_{20}$ blends

expected in the disordered state of a phase when compared to that in its ordered state e.g., the diffusivity of Cu in Zn at 773K in disordered β'-phase ($D_{Cu\,in\,Zn}$=4.8x10^{-13} m^2/s at 773K in β') under identical condition is ~ 35 times higher than that in ordered β($D_{Cu\ in\ Zn}$= 1.4x10^{-14} m^2/s at 773K in β), while the diffusivity of Zn in Cu in disordered β exceeds that in ordered β by about 144 times ($D^{\beta'}_{Zn\ in\ Cu}$=1.3x10^{-11}m^2/s; $D^{\beta}_{Zn\ in\ Cu}$=9.0x 10^{-14}m^2/s at 773K)[263]. Such situation is expected to prevail in the highly disordered AlNi structure as well, which perhaps assist the phase formation reaction by the continuous diffusive mechanism as observed in the present investigation. However, it may be noted that the formation of Nb_3Al during MA follows a continuous diffusive mechanism in spite of it being ordered on MA. It may be noted that the ΔH_f for Nb_3Al is less negative when compared to that of NiAl or $NiAl_3$. The above studies, therefore, indicate that the mode of mixing is continuous diffusive if either ΔH_f > -40kJ mol^{-1} for a given phase or the as milled product is disordered.

5 Kinetics of Alloying during MA

It is well known for over three decades that mechanical deformation enhances the diffusion rate and the process has been termed as "mechanical diffusion" by Balluffi and Rouff[269]. Gleiter[270] has shown that a large potential gradient leads to a high rate of diffusion in the vicinity of a dislocation even at temperatures where self-diffusion is not possible. Gleiter had also shown that the passage of dislocations through Ni_3Al particles in Ni-rich matrix causes pronounced reversal of solute to the matrix from the precipitates, thus resulting in their dissolution at large deformation. Thus, the deformation-enhanced diffusivities can play a significant role in deciding the alloying kinetics during MA.

Recent development of a kinetic model based on a modified version of the iso concentration contour migration (ICCM) method developed earlier[271] to estimate the rate of diffusion controlled dissolution in a two phase planar and multilayered aggregate[268], has been a significant step in kinetic analyses of the MA process. Fig. 23 shows the experimental and calculated results of the respective variation of solubility of Ni, Al and Zn in Cu for $Cu_{50}Ni_{50}$, $Cu_{80}Al_{20}$ and $Cu_{70}Zn_{30}$, as a function of milling time[268]. These experimental results are obtained from the XRD peak shifts of Cu in the above-mentioned elemental blends during MA. The results clearly indicate that the effective mass transport phenomenon operative during MA attains a rate intermediate between that of volume diffusion and grain boundary diffusion. The enhanced diffusion rate in course of MA have been considered to be equivalent to that of volume diffusion at some elevated temperature T_{eff}, that has been determined by comparing the experimental values of solid solution rate with that predicted by the MICCM model. The results of these analyses demonstrate that the equation of ballistic diffusion[62] is not able to account for the extremely large enhancement in the diffusivity values as encountered in MA. It is also clear from the results

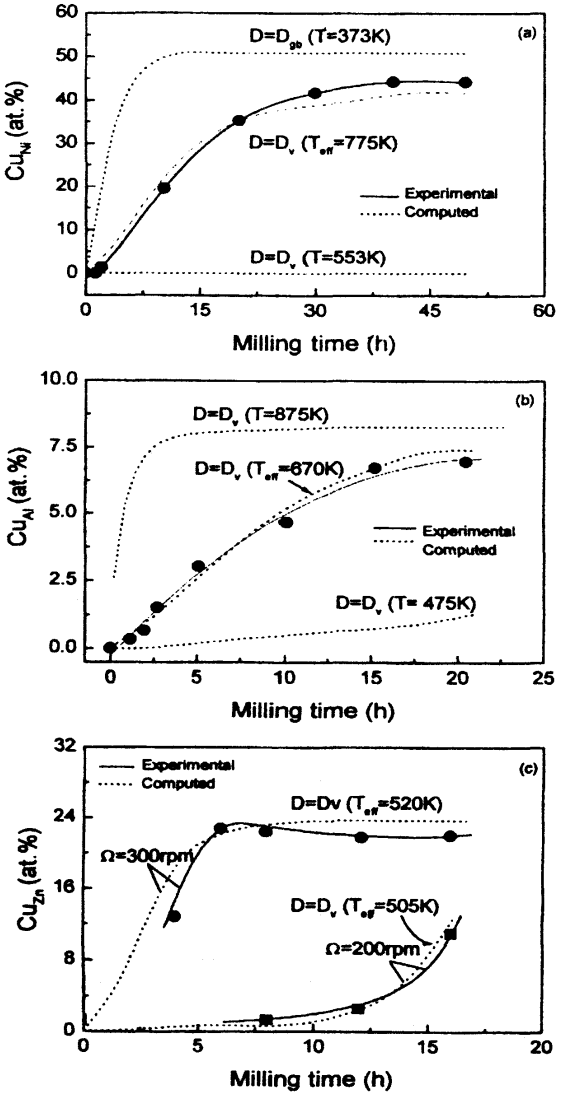

Fig. 23 Experimental and calculated results of the respective variation of solubility of Ni, Al and Zn in Cu for $Cu_{50}Ni_{50}$, $Cu_{80}Al_{20}$ and $Cu_{70}Zn_{30}$, as a function of milling time

Table X

Variation in the T_{eff} and the Homologous Temperature, θ_{eff}, obtained from Experimental Data through MICCM model

Composition	rpm	$T_{solidus}$ (K)	T_{eff} (K)	θ_{eff} (T_{eff}/Tsolidus)
$Cu_{70}Zn_{30}$	200	1190	505	0.42
$Cu_{70}Zn_{30}$	300	1190	520	0.44
$Cu_{60}Zn_{40}$	300	1150	560	0.49
$Cu_{50}Ni_{50}$	300	1533	755	0.49
$Cu_{20}Ni_{80}$	300	1633	785	0.48
$Cu_{80}Al_{20}$	300	1317	670	0.51

of the $Cu_{70}Zn_{30}$ that though the alloying kinetics are remarkably slower at milling disc speed of 200rpm when compared to that at 300rpm in the planetary ball mill P-5, the T_{eff} changes only marginally from 505 to 520K. Furthermore, it is of interest to note that the homologous temperature ($T_{eff}/T_{solidus}$) lies in the range of 0.42 to 0.51 (Table X) in each of these systems, indicating that the effective mass transfer during MA is related to the solidus temperature of the system concerned. It is also evident from these calculations that the crystallite size of the constituent(s) has to be reduced to nanoscale (< 100nm) to achieve any significant rate of alloying by high energy ball milling. It is expected that these results would suffice for predicting the alloying kinetics in diverse systems.

6 Nanocrystallization by Devitrification

Devitrification under controlled conditions has been found to induce nanocrystalline structure[272]. The process may be grouped under two categories depending on the route leading to the nanocrystalline phase evolution *viz.* (i) mechanical deformation induced crystallization and (ii) thermally assisted crystallization of metallic glasses. However, the thermal devitrification has not been discussed here as it is beyond the scope of this review.

The crystallization of amorphous Zr-Ni alloys at higher milling intensities after being amorphized at low intensity milling have been shown by Eckert *et al.*[273] and Trudeau *et al.*,[274] have milled Metglas 2605Co ($Fe_{66}Co_{18}Si_1B_{15}$) and Metglas 2605S-2 ($Fe_{78}Si_9B_{13}$) and found that both crystallize on milling, with Co containing metallic glass crystallizing at shorter milling times. The crystallization of these glasses during milling was attributed to the local rise in the temperature during ball milling, while the early crystallization of the Co containing glass was thought to be due to its lower crystallization temperature (714K as against 826K of Metglas 2605S-2). In an interesting experiment, they[274] have mechanically alloyed Co and Ni to Metglas 2605S and found that Co addition induces rapid crystallization while Ni stabilizes the amorphous phase. This is interesting because Ni addition is known to lower the crystallization temperature to Metglas 2605S to 648K. This work has suggested that a lower crystallization temperature of a metallic glass is not sufficient for it be crystallized during high energy ball milling. Crystallization of metallic glass in Fe-B-Si system by MM has been observed by other several other investigators[275,276]. Enhancement of diffusion due to heavy deformation[277] is also an explanation offered to the nanocrystallization of metallic glasses by high energy ball milling. It appears that temperature rise during milling alone can not explain the crystallization of amorphous phases observed during milling, Chemistry changes during milling and the local temperature rise during milling can enhance the crystallization kinetics. It is possible that the defects introduced during milling accelerate the diffusion and in turn the crystallization kinetics during milling.

7 Nanocrystalline Materials Synthesized by Severe Plastic Deformation

Recent studies have shown that nanocrystalline structure can be synthesized by severe plastic deformation (SPD) either by torsion straining under high pressure (SPTS)[46,278-283] or by equal-channel angular pressing (ECAP)[284-293]. The major advantage of SPD techniques over high energy ball milling and inert gas condensation is that bulk nanocrystalline samples and semi-finished products without any residual porosity can be obtained without the need for compaction and sintering[46]. The concept of ECAP can be traced back to Segal *et al.*,[284] who have pressed the test samples through a die containing two channels, equal in cross section, intersecting at an angle. As

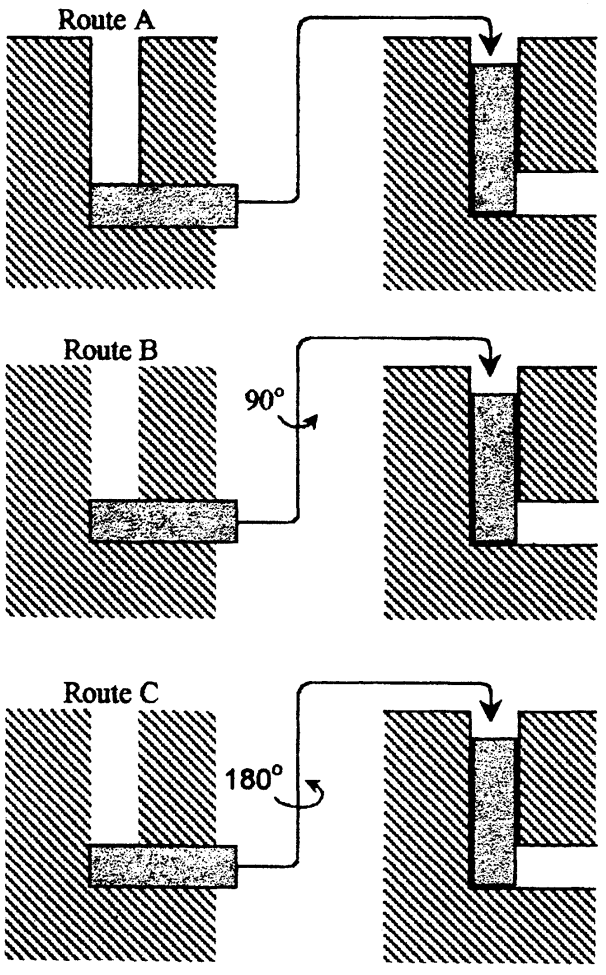

Fig. 24 Schematic of the route adopted during ECAP[293]

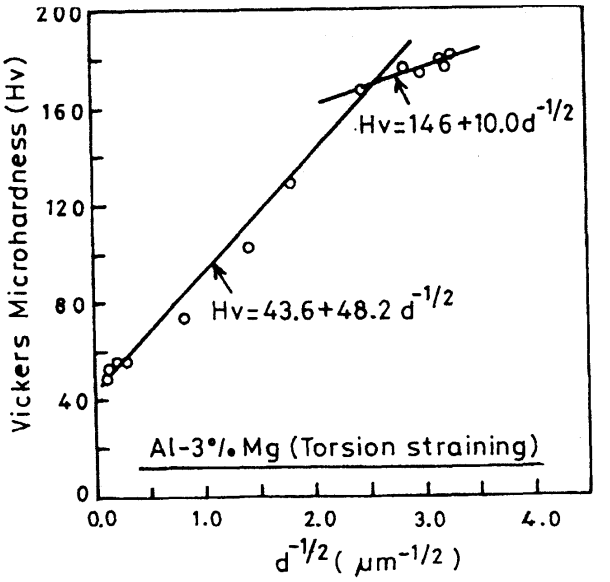

Fig. 25 Change in the microhardness with $d^{-1/2}$ for Al-3%Mg produced by torsion straining[298]

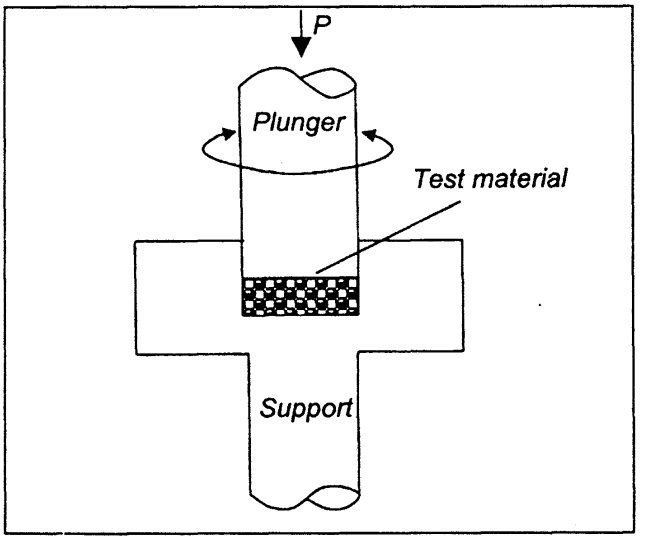

Fig. 26 Schematic of the SPTS route for nanocrystalline structure[46]

a result of pressing the samples undergoes simple shear but retains the same cross section so that the pressing can be repeated for several cycles. The SPD techniques have been shown to produce nanocrystals as small as 50nm[294]. Interestingly, a number of structure insensitive properties such as modulus of elasticity[288], Debye[285] and Curie temperature[287] have been shown to change significantly on nanocrystallization using SPD. Fig. 24[293] shows a schematic of the routes adopted during ECAP. In route A the samples is pressed repetitively without rotation, in route B the samples is rotated by 90° between each pressing and in route C the sample is rotated by 180° between pressings. Nanocrystalline state could be achieved in a number of materials such as Al[295-299], Cu[288,300], Mg[301,302], Ni[303] and intermetallics (γ-TiAl)[291]. It has been shown in case of Al-Mg alloy that the nanocrystalline microstructure developed by ECAP can be useful till $0.5T_m$[296]. Furukawa *et al.*,[297] have shown that the Hall-Petch relation is valid till the finest crystallite size (~90nm) obtained by them by SPD. However, the Hall-Petch slope appears to decrease at fine grain sizes (Fig. 25) which has been attributed to the increased participation of mobile extrinsic dislocations in the boundary regions. An Al-Mg alloy (AZ91) has shown superplasticity with an elongation of 661% and a strain rate sensitivity of 0.3 at $0.5T_m$ after ECAP[302].

The principle of SPTS is illustrated in Fig. 26[46]. In this technique, high hydrostatic pressure of 5-15Gpa is applied at room temperature. An extension of the

solid solubility of Fe in Al to the extent of 2.2wt% has been observed by this technique due to nanocrystallization[283]. This has led to an increase in the microhardness values from 750 to 1750MPa[283]. Subsequent aging at 373K has led to a further increase in the microhardness to 3020MPa due to decomposition of the supersaturated solid solution[283]. A significant increase in the coercivity of Pr-Fe-B-Cu hard magnet has also been observed on SPTS[46].

8 Concluding Remarks

The present paper reviews some of the intriguing facets of the mechanical alloying (MA) and nanostructure formation that have emerged from recent works. The paper highlights the success of MA route in the synthesis of large number of intermetallics and solid solutions in several metallic systems. The works in this field have revealed that the various milling parameters, the milling temperatures, the nature of the product(s) and the presence of more than single phase during MA have a pronounced influence on the limiting grain size attainable by controlling the degree of coalescence of the grains. Present level of work identifies broadly three types of alloying mechanisms, *viz.* continuous diffusive (CD), self-sustaining reactions (SR) and the discontinuous additive (DA) mode. Studies have emphasized the role of enthalpy of formation, ΔH_f, and the ordering characteristics of the phases during alloying in some of the Al and Cu based systems. So far, the DA mechanism is evident only in the case of NiAl and $NiAl_3$ phase formation, having a very highly negative enthalpy (ΔH_f, of -72 and -39kJ mol^{-1} respectively) as well as an ordered structure in the as-milled state, while in the case of rest of the phases CD mechanism is observed. Studies also indicate a switch over from DA to CD mode on disordering of the as-milled NiAl by ternary additions. The kinetic analysis of the phase formation process during MA, on the other hand, shows that the effective mass transfer rate during MA by CD mode attains a value in between the volume diffusion and grain boundary diffusion, and the rate is not so sensitive to the milling intensity. Moreover, this rate in Cu-Ni, Cu-Zn and Cu-Al systems could be correlated with the melting temperature of the systems. It is also revealed that the enhanced rate of mass transfer caused by deformation during MA is inexplicable by the existing ballistic diffusion model. The success and advantages of the recently developed mechanical methods of porosity-free bulk nanostructure production *viz.* severe plastic deformation by torsion straining (STPS) and by equal-channel angular pressing (ECAP) have also been reviewed.

References

1 H Gleiter *Prog Mater Sci* **33** (1989) 223

2 B H Kear, R W Siegel and T Tsakalakos (Eds.) Proc First Int Conf Nanostructured Materials 1992 *Nanostructured Mater* **2** (1993)

3 H E Schaefer, R Wurschum, H Gleiter and T Tsakalakos (Eds.) Proc Second Int Conf on Nanostructured Materials 1994 *Nanostructured Mater* **6** (1995)

4 M L Trudeau, V Provenzano, R D Shull and J Y Ying Proc Third Int Conf on Nanostructured Materials (Nano'96) 1996 in *Nanostructured Mater* **9** (1997)

5 Nano'98

6 Nano'2000

7 L E McCandlish, B H Kear, D E Polk and R W Siegel (Eds.) MRS Symp Proc on Multicomponent Ultrafine Microstructures, Pittsburgh (PA), MRS **132** (1989)

8 D C V Aken (Ed.) *Symp Proc Microcomposites and Nanophase Materials* Warrendale (PA) TMS (1991)

9 G Kostorz, I Gorynin and V Trefilev (Eds.) Symp Proc Materials under Extreme Conditions and Nanophase Materials 1992 *Mater Sci Eng A* **168** (1993)

10 S Komarneni, J C Parker and G J Thomas (Eds.) MRS Symp. Proc Nanophase and Nanocomposite Materials Pittsburgh (PA) MRS **286** (1993)

11 R D Shull (Ed.) Symp Proc Nanophase and Nanocrystalline Structure Warrendale (PA) TMS (1993)

12 R D Shull (Ed.) Proc of Special Symp on Nanocrystalline Materials New York (NY) Pergamon Press (1993)

13 R D Shull and J M Sanchez (Eds.) Symp Proc on Nanophase and Nanocrystalline Materials Warrendale (PA) TMS (1994)

14 G C Hadjipanayis and R W Siegel (Eds.) Symp Proc on *Nanophase Materials - Structure, Properties and Applications* Kluwer Netherlands (1994)

15 R D Shull (Ed.) *Symp Proc on Structure and Properties of Nanophase Materials* 1995 *Nanostructured Mater* **7** (1996)

16 C Suryanarayana, J Singh and F H Froes (Eds.) *Symp Proc Processing and Properties of Nanocrystalline Materials* Warrendale (PA) TMS (1996)

17 D L Bourell (Ed.) *Symp Proc Synthesis and Processing of Nanocrystalline Powder* Warrendale (PA) TMS (1996)

18 C Suryanarayana *Bull Mater Sci* **17** (1994) 307

19 H Gleiter *Nanostructured Mater* **1** (1992) 1

20 H Gleiter *Nanostructured Mater* **6** (1995) 3

21 R W Siegel *Mater Sci Eng A* **168** (1993) 189

22 C Suryanarayana *Int Mater Rev* **40** (1995) 41

23 R Birringer *Mater Sci Eng A* **117** (1989) 33

24 R W Siegel *Ann Rev Mater Sci* **21** (1991) 559

25 V G Gryaznov and L I Trusov *Prog Mater Sci* **37** (1993) 289

26 C Suryanarayana and F H Froes *Metall Trans A* **23** (1992) 1071

27 R W Siegel *Nanostructured Mater* **4** (1994) 121

28 M N Ritter and T Abraham *Int J Powder Metall* **34** (1998) 33

29 J S Benjamin *Metall Trans* **1** (1970) 2943

30 C C Koch, O B Cavin, C G Mckamey and J O Scorbrough *Appl Phys Lett* **43** (1983) 1017

31 H J Fecht, E Hellstern, Z Fu and W L Johnson *Metall Trans A* **21** (1990) 2333

32 C C Koch *Materials Science and Technology – A Comprehensive Treatment* (Ed. R W Cahn) Weinheim VCH **15** (1991) 193

33 S K Pabi and A Das, *Metals Mater Processes* **9** (1997) 229

34 B S Murty and S Ranganathan *Int Mater Rev* **43** (1998) 101

35 C C Koch *Nanostructured Mater* **2** (1993) 109

36 A R Yavari *Mater Trans JIM* **36** (1995) 228

37 E Gaffet, M Abdellaoui and N M Gaffet *Mater Trans JIM* **36** (1995) 198

38 H J Fecht *Nanostructured Mater* **1** (1992) 125

39 C C Koch and Y S Cho *Nanostructured Mater* **1** (1992) 207

40 H J Fecht *Nanostructured Mater* **6** (1995) 33

41 C C Koch *Nanostructured Mater* **9** (1997) 13

42 C C Koch *Mater Sci Eng A* **244** (1998) 39

43 C C Koch and J D Whittenberger *Intermetallics* **4** (1996) 339

44 D A Rigney *Ann Rev Mater Sci* **18** (1988) 141

45 A E Berkowitz and J L Walter *J Mater Res* **2** (1987) 277

46 V V Stolyarov and R Z Valiev *Mater Sci Forum* **307** (1999) 185

47 M Atzmon, J D Veerhoven, E D Gibson and W L Johnson *Appl Phys Lett* **45** (1984) 1052

48 L Schultz *Rapidly Quenched Metals* V (Eds. S Steeb and H Warlimont) Amsterdam North-Holland (1984) 1585

49 A Sagel, H Sieber, H J Fecht and J H Perepezko *Acta Mater* **46** (1998) 4233

50 F Boordeaux and A R Yavari *J Appl Phys* **67** (1990) 2385

51 A Calka and A P Radlinski *Mater Sci Eng* A **134** (1991) 1350

52 V Arnhold, J Baumgarten and H C Neubing *Proc World Conf Powder Metallurgy* (PM'90), London UK The Institute of Metals 2 (1990) 259

53 W E Kuhn, I L Friedman, W Summers and A Szegvari *Metals Handbook, Powder Metallurgy* Metals Park Ohio ASM 7 (1985) 56

54 I Kerr *Metal Powder Rep* **48** (1993) 36

55 R B Schwarz and C C Koch *Appl Phys Lett* **49** (1986) 146

56 M Abdellaoui and E Gaffet *J All Comp* **209** (1994) 351

57 M Abdellaoui and E Gaffet *Acta Metall Mater* **43** (1995) 1087

58 T H Courtney *Mater Trans JIM* **36** (1995) 110

59 M Magini and A Iasonna *Mater Trans JIM* **36** (1995) 123

60 T H Courtney and D Maurice *Scripta Mater* **34** (1996) 5

61 E Gaffet, N Malhouroux and M Abdellaoui *J All Comp* **194** (1993) 339

62 R Watanabe, H Hashimoto and G G Lee *Mater Trans JIM* **36** (1995) 102

63 E Gaffet *Mater Sci Eng A* **132** (1991) 181

64 C Suryanarayana and F H Froes *J Mater Res* **5** (1990) 1880

65 A Calka and A P Radlinski *Appl Phys Lett* **58** (1991) 119

66 A W Weeber, A J H Wester, W J Haag and H Bakker *Physica B* **145** (1987) 349

67 M S El-Eskandarany, K Aoki and K Suzuki *J Less Common Metals* **167** (1990) 113

68 M Abdellaoui and E Gaffet *Acta Metall Mater* **44** (1996) 725

69 D Basset, P Matteazzi and F Miani *Mater Sci Eng A* **168** (1993) 149

70 T Aizawa, K Tatsuzawa and J Kihara *Proc 1993 Powder Metallurgy World Congress* (Eds. Y Bando and K Kosuge) Kyoto Japan *Jap Soc Powder and Powder Metallurgy* (1993) 96

71 M Martin and E Gaffet *Colloque de Phys* **51** (1990) 71

72 E Hellstern, H J Fecht, C Garland and W L Johnson *J Appl Phys* **65** (1989) 305

73 E Hellstern, H J Fecht, C Garland and W L Johnson *MRS Symp Proc* **132** (1989) 137

74 J Eckert, J C Holzer, C E Krill III and W L Johnson *J Mater Res* **7** (1992) 1992

75 D Oleszak and P H Shingu *J Appl Phys* **79** (1996) 2975

76 J Joardar, S K Pabi and B S Murty *Proc Int Conf on Recent Adv Metallur Process* (Eds. D H Sastry, E S Dwarakadasa, G N K Iyengar and S Subramanian) New Age Int Publ New Delhi India **1** (1997) 647

77 G B Schaffer and J S Forrester *J Mater Sci* **32** (1997) 3157

78 B S Murty, J Joardar and S K Pabi *Nanostructured Mater* **7** (1996) 691

79 B S Murty, D Das, I Manna and S K Pabi *Acta Mater* (Communicated)

80 S K Pabi, J Joardar and B S Murty *J Mater Sci* **31** (1996) 3207

81 K H S Singh *Production of Nanocrystalline Nickel Aluminides by Mechanical Alloying* M Tech Thesis, Indian Institute of Technology Kharagpur India (1995)

82 R Birringer *Mater Sci Eng A* **117** (1989) 33

83 R D Noebe, R R Bowman and M V Nathal *Int Mater Rev* **38** (1993) 193

84 D B Miracle *Acta Metall Mater* **41** (1993) 649

85 S K Pabi, D Das, T K Mahapatra and I Manna *Acta Mater* **41** (1998) 3501

86 K Yamada and C C Koch *J Mater Res* **8** (1993) 1317

87 T D Shen and C C Koch *Mater Sci Forum* **179-181** (1995) 17

88 D K Pathak, Ph D Thesis North Carolina State University Raleigh USA (1995)

89 R L White Ph D Thesis Stanford University Stanford USA (1979)

90 R M Davis M S Thesis North Carolina State University Raleigh USA (1987)

91 B T Mcdermott M S Thesis North Carolina State University Raleigh USA (1988)

92 H Kimura and M Kimura *Solid State Powder Processing* (Ed. A H Clauer and J J Debarbadillo) Warrendale (PA) TMS-AIME (1990) 365

93 A B Borzov and E Y Kaputkin *Mechanical Alloying Structural Applications* (Eds. J J deBarbadillo and A H Clauer) Addendum Materials Park Ohio ASM International (1993)

94 C C Koch *Int J Mechanochem Mech Alloying* **1** (1994) 56

95 E T B Levinson, A A Kolesnikov and I V Fine *Mater Sci Forum* **88-90** (1992) 113

96 A E Yermakov, E E Yurchikov and V A Barinov *Phys Met Metall* **52** (1981) 50

97 A E Yermakov, V A Barinov and E E Yurchikov *Phys Met Metall* **54** (1982) 935

98 R M Davis and C C Koch *Scripta Metall* **21** (1987) 305

99 D R Maurice and T H Courtney *Metall Trans* A **21** (1990) 289

100 M Magini, N Burgio, A Iasonna, S Martelli, F Padella and E Paradiso *J Mater Syn Proc* **1** (1993) 135

101 A K Bhattacharya and E Arzt *Scripta Metall Mater* **27** (1992) 749

102 P J Miller, C S Coffey and V F Devost *J Appl Phys* **59** (1986) 913

103 J S Benjamin *Sci Am* **234** (1976) 40

104 W Schlump and H Grewe *New Materials by Mechanical Alloying* (Eds. E Arzt and L Schultz) Oberursel Germany Deutsch Gesellschaft Fuer Metallkunde (1989) 307

105 L Schultz *Mater Sci Eng A* **97** (1988) 15

106 H J Fecht, E Hellstern, Z Fu and W L Johnson *Metall Trans A* **21** (1990) 2333

107 T R Malow and C C Koch *Acta Mater* **45** (1997) 2177

108 C Moelle and H J Fecht *Nanostructured Mater* **6** (1995) 421

109 R Z Valiev, R S Mishral, J Grozal and A K Mukherjee *Scripta Mater* **34** (1996) 1443

110 J Xu, J S Yin and E Ma *Nanostructured Mater* **8** (1997) 91

111 E Gaffet and M Harmelin *J Less Common Metals* **157** (1990) 201

112 T D Shen, C C Koch, T L McCormick, R J Nemanich, J Y Huang and J P Huang *J Mater Res* **10** (1995) 139

113 T D Shen, W Q Ge, K Y Wang, M X Quan, J T Wang, W D Wei and C C Koch *Nanostructured Mater* **7** (1996) 393

114 H Hermann, T Schubert, W German and N Maltern *Nanostructured Mater* **8** (1997) 215

115 B E Warren and B L Averback *J Appl Phys* **21** (1950) 595

116 G K Williamson and W H Hall *Acta Metall* **1** (1953) 22

117 T G Nieh and J Wadsworth *Scripta Metall Mater* **25** (1991) 955

118 J Eckert, J C Holzer, C E Krill III and W L Johnson *J Mater Res* **7** (1992) 1980

119 T D Shen and C C Koch *Acta Mater* **44** (1996) 753

120 M Oehring and R Bormann *Mater Sci Eng A* **134** (1991) 1330

121 B S Murty, M Mohan Rao and S Ranganathan *Nanostructured Mater* **3** (1993) 459

122 B S Murty, M D Naik, S Ranganathan and M Mohan Rao *Mater Forum* **16** (1992) 19

123 R Nagarajan, B S Murty and S Ranganathan *Chinese J Mater Res* (1994) 215

124 T B Massalski (Ed) Binary Alloy Phase Diagrams ASM Metals Park OH (1986)

125 K Uenishi, K F Kobayashi, K N Ishihara and P M Shingu *Mater Sci Eng A* **134** (1991) 1342

126 F H Froes, C Suryanarayana, K Russell and C G Li *Mater Sci Eng A* **192/193** (1995) 612

127 K F Kobayashi, N Tachibana and P H Shingu *J Mater Sci* **25** (1990) 3149

128 C Suryanarayana and R Sundaresan *Mater Sci Eng A* **131** (1991) 237

129 C Suryanarayana *Metals and Mater* **2** (1996) 195

130 T Tanaka, K N Ishihara and P H Shingu *Metall Trans A* **23** (1992) 2431

131 J Eckert, L Schultz and K Urban *Europhys Lett* **13** (1990) 349

132 J Y Huang, Y D Yu, Y K Wu, D X Li and H Q Ye *J Mater Res* **12** (1997) 936

133 S Enzo, R Frattini, R Gupta, P P Marci, G Principi, L Schiffini and G Scipione *Acta Mater* **44** (1996) 3105

134 A Hightower, B Fultz and R C Bowman Jr *J All Comp* **252** (1997) 238

135 M Abdellaoui, T Barradi and E Gaffet *J All Comp* **198** (1993) 155

136 M Abdellaoui, C M Djega and E Gaffet *J All Comp* **259** (1997) 241

137 V K Portnoy, V I Fadeeva and I N Zaviyalova *J All Comp* **224** (1995) 159

138 G Walkowiak, T Sell and H Mehrer *Z Metallkde* **85** (1994) 332

139 M Hida, K Asai, Y Takemoto and A Sakakibara *Mater Sci Forum* **235-238** (1997) 187

140 H J Fecht, G Han, Z Fu and W L Johnson *J Appl Phys* **67** (1990) 1744

141 B S Murty and S K Pabi *(unpublished work)*

142 K Uenishi, K F Kobayashi, K Nasu, H Hatemo, K N Ishihara and P M Shingu *Z Metallkde* **83** (1992) 132

143 A R Yavari, P J Desre and T Benameur *Phys Rev Lett* **68** (1992) 2235

144 J Eckert, J C Holzer, C E Krill III and W L Johnson *J Appl Phys* **73** (1993) 2794

145 E Ma, M Atzmon and F E Pinkerton *J Appl Phys* **74** (1993) 955

146 E Gaffet, M Harmelin and F Faudot *J All Comp* **194** (1993) 23

147 J Y Huang, A Q He, Y K Wu, H Q Ye and D X Li *J Mater Sci* **31** (1996) 4165

148 B Mazumdar, M M Raja, A Narayanaswamy and K Chattopadhyay *J All Comp* **248** (1997) 192

149 E Gaffet, C Louison, M Hermelin and F Faudot *Mater Sci Eng A* **134** (1991) 1380

150 C S Xiong, Y H Xiong, H Zhu, T F Sun, E Dong and G X Liu *Nanostructured Mater* **5** (1995) 425

151 F Fukunaga, M Mori, K Inoue and M Mizutani *Mater Sci Eng A* **134** (1991) 863

152 K Sakurai, M Mori and U Mizutani *Phys Rev B* **46** (1992) 5711

153 K Sakurai, Y Yanada, C H Lee, T Fukunaga and U Mizutani *Mater Sci Eng A* **134** (1991) 1414

154 G Veltl, B Scholz and H D Kunze *Mater Sci Eng A* **134** (1991) 1410

155 T Fukunaga, K Nakamura, K Suzuki and U Mizutani *J Non-Cryst Sol* **117/118** (1990) 700

156 J G C Moreno, V M Lopez, H H A Calderon and J C Angels *Scripta Metall Mater* **28** (1993) 645

157 M Baricco, N Cowlam, L Schiffini, P P Maira, R Frattini and S Enzo *Phil Mag B* **68** (1993) 957

158 C Gente, M Oehring and R Bormann *Phys Rev A* **48** (1993) 13244

159 J Y Huang,, Y K Wu, A Q He and H Q Ye *Nanostructured Mater* **4** (1994) 293

160 A R Yavari *Mater Sci Eng A* **179/180** (1994) 20

161 J Y Huang, A Q He and Y K Wu *Nanostructured Mater* **4** (1994) 1

162 B L Huang, R J Perez, E J Lavernia and M J Luton *Nanostructured Mater* **7** (1996) 69

163 J Y Huang, Y D Yu, Y K Wu, D X Li and H Q Ye *Acta Mater* **45** (1997) 113

164 R Bohn, T Hanbold, R Birringer and H Gleiter *Scripta Metall Mater* **25** (1991) 811

165 J S C Jang and C C Koch *Scripta Metall Mater* **24** (1990) 1599

166 S Dymek, M Dollar, S J Hwang and P Nash *Mater Sci Eng A* **152** (1992) 160

167 M Jain and T Christman *Acta Metall Mater* **42** (1994) 1901

168 E Ivanov, T Grigorieva, G Gdubkova, V Boldyrev, A B Fasman, S D Mikhailenko and O T Kalimna *Mater Lett* **7** (1988) 51

169 B S Murty, K H S Singh and S K Pabi *Bull Mater Sci* **19** (1996) 565

170 M Atzmon *Phys Rev Lett* **64** (1990) 487

171 T Itsukaichi, M Umemoto and J G C Moreno *Scripta Metall Mater* **29** (1993) 583

172 F Cardellini, G Mazzone, A Montone and M V Antisari *Acta Metall Mater* **42** (1994) 2445

173 B L Huang, J Vallone and M J Luton *Nanostructured Mater* **5** (1995) 411

174 R Maric, K N Ishihara and P H Shingu *J Mater Sci Lett* **15** (1996) 1180

175 Z G Liu, J T Guo and Z A Hu *Mater Sci Eng A* **192/193** (1995) 577

176 S K Pabi and B S Murty *Mater Sci Eng A* **214** (1996) 146

177 M Oehring, Z H Yan, H Klassen and R Bormann *Phys Stat Solidi (a)* **131** (1992) 671

178 B S Murty Ph D Thesis Indian Institute of Science Bangalore India (1992)

179 R C Baun, P K Mirchandani and A S Watwe *Proc Mod Dev Powder Metallurgy* APMI **18** (1988) 479

180 K Y Lee, H K Cho and J H Ahn *J Mater Sci Lett* **15** (1996) 1324

181 C Suryanarayana, G H Chen, A Frefer and F H Froes *Mater Sci Eng A* **158** (1992) 93

182 W Guo, S Martelli, N Burgio, M Magini, F Padella, E Padadiso and I Soleta *J Mater Sci* **26** (1990) 6190

183 Y H Park, H Hashimoto and R Watanabe *Mater Sci Forum* **88-90** (1992) 59

184 C Suryanarayana, R Sundaresan and F H Froes *Mater Sci Eng A* **150** (1992) 117

185 M A Morris and D G Morris *Mater Sci Eng A* **136** (1991) 59

186 M A Morris and D G Morris *Mater Sci Forum* **88-90** (1992) 529

187 G H Fair and J V Wood *Powder Metall* **36** (1993) 123

188 F Cardellini, V Contini and G Mazzone *J Mater Sci* **31** (1996) 4175

189 F R de Boer, R Boom, W C M Mattens, A R Miedema and A K Niessen *Cohesion in Metals - Transition Metal Alloys Cohesion and Structure* (Eds. F R deBoer and D G Pettifor) North-Holland Publications Co Amsterdam Holland 1 (1988)

190 L M Di, H Bakker and F R de Boer *Physica B* **182** (1992) 91

191 S X J Zhou, D Zhang and X Wang *Mater Lett* **26** (1996) 245

192 R B Schwarz, S Srinivasan and P B Desch *Mater Sci Forum*, **88-90** (1992) 595

193 D C Crew, P G Mccormic and R Street *Scripta Metall Mater* **32** (1995) 315

194 M R Pachauri, D L Zhang and T B Massalski *Mater Sci Eng A* **174** (1994) 119

195 Z Zdujic, D Poleti, L Karanovic, K F Kobayashi and P H Shingu *Mater Sci Eng A* **185** (1994) 77

196 Z Peng, C Suryanarayana and F H Froes *Metall Mater Trans A* **27** (1996) 41

197 H J Ahn and K Y Lee *Mater Trans JIM* **36** (1995) 297

198 S Kawanashi, K Ionishi and K Okazaki *Mater Trans JIM* **34** (1993) 43

199 J Saida, Y Tanaka and K Okazaki *Mater Trans JIM* **37** (1996) 265

200 C Rock and K Okazaki *Nanostructured Mater* **5** (1995) 643

201 L Schultz, E Hellstern and G Zorn *Z Phys Chem* **157** (1988) 203

202 H Schropf, C Kuhrt, E Arzt and L Schultz *Scripta Metall Mater* **30** (1994) 1569

203 J G C Moreno, T Itsukaichi and M Umemoto *Mater Sci Eng A* **181/182** (1994) 1202

204 C Suryanarayana, W Li and F H Froes *Scripta Metall Mater* **31** (1994) 1465

205 G H Chen, C Suryanarayana and F H Froes *Scripta Metall* **25** (1991) 2537

206 R Radhakrishnan, S Bhaduri and C H Hanegar Jr *J Metals* **49** (1997) 41

207 A P Radlinski and A Calka *Mater Sci Eng A* **134** (1991) 1376

208 K Omuro and H Miura *J Appl Phys* **30** (1991) L851

209 M K Datta, S K Pabi and B S Murty *(unpublished work)*

210 M Gaffet and E Gaffet *J All Comp* **198** (1993) 143

211 A G Escorial, P Adveda, M C Cristina, A Martin, F Carmona, F Cebollada, V E Martin, M Leonato and J M Gonzalez *Mater Sci Eng A* **134** (1991) 1394

212 O Kohmoto, N Yamaguchi and T Mori *J Mater Sci* **29** (1994) 3221

213 M Abdellaoui, E Gaffet, T Barradi and F Faudot *IEEE Trans Mag* **30** (1994) 4887

214 M Umemoto *Mater Trans JIM* **36** (1995) 373

215 G Veltl, B Scholz and H D Kunze *New Materials by Mechanical Alloying* (Eds. E Arzt and L Schultz) Deutsch Gesellschaft fur Metallkunde Oberursel Germany (1989) 79

216 D Parlapanski, S Denev, S Ruseva and E Gatev *J Less Common Metals* **171** (1991) 231

217 M Oehring and R Bormann *Mater Sci Eng A* **134** (1991) 1330

218 H Park, H Hashimoto and R Watanabe *Mater Sci Eng A* **181/182** (1994) 1212

219 N Zotov and D Parlapanski *J Mater Sci* **29** (1994) 2813

220 R B Schwarz, S R Srinivasan, J J Petrovic and C J Maggiore *Mater Sci Eng A* **155** (1992) 75

221 L Liu, F Padella, W Guo and M Magini *Acta Metall Mater* **43** (1995) 3755

222 P Y Lee, T R Chen, J L Yang and T S Chin *Mater Sci Eng A* **192/193** (1995) 556

223 J Liu and M Magini *J Mater Res* **12** (1997) 2281

224 M Magini, N Basili, N Burgio, G Ennas, S Martelli, F Padella, E Paradiso and P Susini *Mater Sci Eng A* **134** (1991) 1406

225 T Nasu, K Nagaoka, T Takahashi, T Fukunaga and K Suzuki *Mater Trans JIM* **30** (1989) 146

226 D L Zhang and T B Massalski *J Mater Res* **9** (1994) 53

227 R K Viswanandhan, S K Mannan and S Kumar *Scripta Metall* **22** (1988) 1011

228 T Lou, G Fau, B Ding and Z Hu *J Mater Res* **12** (1997) 1172

229 K S Kumar and S K Mannan *MRS Symp Proc MRS* Pittsburgh PA **133** (1989) 415

230 B T Mcdermott and C C Koch *Scripta Metall* **20** (1986) 669

231 F Cardellini, V Contini, G Mazzone and M Vittori *Scripta Metall Mater* **28** (1993) 1035

232 H Kimura, M Kimura and F Takada *J Less Common Metals* **140** (1988) 113

233 R L White and W D Nix *New Developments and Applications in Composites*, (Eds. D K Wilsdorf and W C Harrigan) Warrendale (PA) TMS (1979) 78

234 M S Kim and C C Koch *J Appl Phys* **62** (1987) 3450

235 T Tanaka, K N Ishihara and P H Shingu *Metall Trans A* **23** (1992) 2431

236 K Tokumitsu *Mater Sci Forum* **235-238** (1997) 127

237 L Li and J Jang *J All Comp* **209** (1994) L1

238 H Huang and P G Mccormick *J All Comp* **256** (1997) 258

239 M A Morris and D G Morris *Solid State Powder Processing* (Eds. A H Clauer and J J Debarbadillo) Warrendale (PA) TMS-AIME, 299 (1990)

240 C W Pan, M P Hung and Y H Chang M*ater Sci Eng A* **185** (1994) 147

241 L B Hong, C Bausal and B Fultz *Nanostructured Mater* **4** (1994) 949

242 M L Trudeau, R Schulz, L Zaluski, S Hosatte, D H Ryan, C B Doner, P Tessier, J O Strom-Olsen and A V Neste *Mater Sci Forum* **88-90** (1992) 537

243 C R Clark, C Wright, C Suryanarayana, E G Baburaj and F H Froes *Mater Lett* **33** (1997) 71

244 L Aymard, M Ichitsubo, K Uchida, E Sekreta and F Ikazaki *J All Comp* **259** (1997) L5

245 A Corrias, G Ennas, G Morangiu, A Musinu, G Paschina and D Zedda *Mater Sci Eng A* **204** (1995) 211

246 M S El-Eskandarany *Metall Mater Trans A* **27** (1996) 2374

247 A Teresiak, N Mattern, H Kubsch and B F Kieback *Nanostructured Mater* **4** (1994) 775

248 L L Ye, J Y Huang, Z G Liu, M X Quan and Z Q Hu *J Mater Res* **11** (1996) 2092

249 Z H Yan, M Oehring and R Bormann *J Appl Phys* **72** (1992) 2478

250 M A Morris *J Mater Sci* **26** (1991) 1157

251 M Zhu, B L Li, Y Gao, L Li, K C Luo, H X Sui and Z X *Scripta Metall Mater* **36** (1997) 447

252 V Provenzano and R L Holtz *Mater Sci Eng A* **204** (1995) 125

253 Y Du, S Li, K Zhang and K Lu *Scripta Metall Mater* **36** (1997) 7

254 J Naser, W Reinhemann and H Ferkel *Mater Sci Eng A* **234** (1997) 467

255 N Q Wu, J M Wu, G X Wang and Z Z Li *Mater Lett* **32** (1997) 259

256 K Liu, J Zhang, J Wang and G Chen *Scripta Metall Mater* **36** (1997) 1113

257 O N Senkov, F H Froes and E G Baburaj *Scripta Mater* **37** (1997) 575

258 T Kaneyoshi, T Takahashi, Y Hayashi and M Motayama(Eds. E D Capus and R M German) *Proc 1992 Powder Metallurgy World Congress* New Jersey Metal Powder Industries Federation 7 (1992) 421

259 I Manna, P P Chatterjee, V Srinivasa Rao and S K Pabi *Scripta Mater* **40** (1999) 409

260 Th Pfullmann, M Oehring, R Bohn and R Bormann *Mater Sci Forum* **225-227** (1996) 757

261 A K Bhattacharya and E Arzt *Scripta Metall Mater* **27** (1992) 635

262 J Zbiral, G Jangg and G Korb *Mater Sci Forum* **88-90** (1992) 19

263 R C Weast (Ed) CRC Handbook of Chemistry and Physics 58th Edn CRC Press Ohio (1977) F-62

264 S K Pabi, J Joardar, I Manna and B S Murty *Nanostructured Mater* **9** (1997) 149

265 Z G Liu, J T Guo, L L He and Z Q Hu *Nanostruct Mater* **7** (1994) 787

266 K A Philpot, Z A Munir and J B Holt *J Mater Sci* **22** (1987) 159

267 U A Tamburini and Z A Munir *J Appl Phys* **66** (1989) 5039

268 S K Pabi, I Manna and B S Murty *Bull Mater Sci* **22** (1999) 101

269 R W Balluffi and A L Rouff *Appl Phys Lett* **1** (1962) 59

270 H Gleiter *Acta Metall* **16** (1967) 455

271 S K Pabi *Phys Status Solidi (a)* **51** (1979) 281

272 K Lu, *Mater Sci Eng R* **16** (1996) 161

273 J Eckert, L Schultz and E Hellstern *J Appl Phys* **64** (1988) 3224

274 M L Trudeau, R Schulz, D Dusault and A V Neste *Phys Rev Lett* **64** (1990) 99

275 C Bansal, B Fultz and W L Johnson *Nanostructured Mater* **4** (1994) 919

276 B Huang, R J Perez, P J Crawford, A A Sharif, S R Nutt and J Lavernia *Nanostructured Mater* **5** (1995) 545

277 M L Trudeau *Appl Phys Lett* **64** (1994) 3661

278 R Sh Musalimov and R Z Valiev *Scripta Metall Mater* **27** (1992) 1685

279 R Z Valiev, A V Koznikov and R R Mulyukov *Mater Sci Eng A* **168** (1993) 141

280 J Languillaume, F Chemilik, G Kapelski, F Bordeaux, A A Nazarov, G Canova, C Esling, R Z Valiev and B Baudelet *Acta Mater* **41** (1993) 2953

281 Y Ma, Z Horita, M Furukawa, M Nemoto, R Z Valiev and T G Langdon *Mater Lett* **23** (1995) 283

282 Y V Ivanisenko, A V Korznikov, I M Safarov and R Z Valiev *Nanostructured Mater* **6** (1995) 433

283 O N Senkov, F H Froes, V V Stolyarov, R Z Valiev and J Liu *Nanostructured Mater* **10** (1998) 691

284 V M Segal, V I Rexnikov, A E Drobyshevsky and V I Kopylov *Russian Metallurgy* **1** (1981) 99

285 R Z Valiev, R R Mulyukov, V V Ovchinnikov and V A Shabashov *Scripta Metall Mater* **25** (1991) 841

286 N A Akhmadeev, V I Kopylov, R R Mulyukov and R Z Valiev Izvest Akad Nauk SSSR *Metally* **5** (1992) 96

287 K Y Mulyukov, S B Kaphizov and R Z Valiev *Phys Status Sol (a)* **133** (1992) 447

288 N A Akhmadeev, N P Kobelev, R R Mulyukov, Y M Soifer and R Z Valiev *Acta Metall Mater* **41** (1993) 1041

289 J Wang, Z Horita, M Furukawa, M Nemeto, N K Tsenev, R Z Valiev, Y Ma and T G Langdon *J Mater Res* **8** (1993) 2810

290 V M Segal *Mater Sci Eng A* **197** (1995) 157

291 S L Semiatin, V M Segal, R L Goetz, R E Goforth and T Hartwig *Scripta Metall Mater* **33** (1995) 535

292 Y Iwahashi, J Wang, Z Horita, M Nemoto and T G Langdon *Scripta Mater* **35** (1996) 143

293 Y Iwahashi, Z Horita, M Nemoto and T G Langdon, *Acta Mater* **46** (1998) 3317

294 R Z Valiev and R Sh Musalimov *Phys Metal Metall* **78** (1994) 666

295 J Wang, M Furukawa, Z Horita, M Nemeto, R Z Valiev and T G Langdon *Mater Sci Eng A* **216** (1996) 41

296 J Wang, Y Iwahashi, Z Horita, M Furukawa, M Nemeto, R Z Valiev and T G Langdon *Acta Mater* **44** (1996) 2973

297 M Furukawa, Z Horita, M Nemeto, R Z Valiev and T G Langdon *Acta Mater* **44** (1996) 4619

298 M Kawazoe, T Shibata, T Mukai and K Higashi *Scripta Mater* **36** (1997) 699

299 Y Iwahashi, Z Horita, M Nemeto and T G Langdon *Acta Mater* **45** (1997) 4733

300 R Z Valiev, E V Kozlov, Y F Ivanov, J Lian A A Nazarov and B Baudelet *Acta Metall Mater* **42** (1994) 2467

301 M Mabuchi, H Iwasaki and K Higashi *Mater Sci Forum* **243-245** (1997) 547

302 M Mabuchi, H Iwasaki, K Yanase and K Higashi *Scripta Mater* **36** (1997) 681

303 V M Segal *Mater Sci Eng A* **197** (1995) 157